Cooperative Routing in Wireless Ad Hoc Networks

CHEUNG, Man Hon

A Thesis Submitted in Partial Fulfilment
of the Requirements for the Degree of
Master of Philosophy
in
Information Engineering

August 2007

摘要

在無線自組織網絡(wireless ad hoc network)的設計中，其中一項最大的挑戰便是有限的能量供應。在本論文裡，我們根據瑞利衰落(Rayleigh fading)和脈衝位置調制(Pulse Position Modulation)-跳時(Time Hopping)-超寬帶(Ultra-Wideband)無線通訊兩種物理層(physical layer)模型去設計協同路由(cooperative routing)和干擾受限環境路由(interference-aware routing)的算法(algorithm)，以減低能量的消耗。

在瑞利衰落協同路由這部份，每一跳(hop)都可以有兩個節點(node)傳送給接收機，而每一跳的傳送能量都是一樣的。兩個節點與接收機的距離一般而言都是不同的。為了降低中斷概率(probability of outage)，我們決定兩個節點應該何時合作和對應的能量分配比例。中斷概率的定義是訊噪比(signal-to-noise ratio)少於某個特定的起點 Θ。接著，我們把協同和非協同方案放在一維泊松(Poisson)隨機網絡和二維格子網絡進行分析和仿真。之後，我們提出了一個協同路由的算法，並在二維隨機網絡裡進行仿真。結果顯示以上協同方案的分集階數(diversity order)都為二。

在超寬帶無線通訊這部份，我們首先算出犁耙式接收機(Rake receiver)在加性白高斯噪音(Additive White Gaussian Noise)和多用戶干擾(Multi-User Interference)下的誤碼率(bit error rate)。根據這結果，我們提出一個合適的鏈路成本因子(link cost)和最優干擾受限環境路由算法，藉以找出一條既能符合誤碼率要求，又能使用最少能量傳送每位元的路由。我們也提出了一個簡化的干擾受限環境路由算法。結果顯示我們的干擾受限環境路由算法比其他路由算法節省更多的傳送能量。

接著，我們提出一個應用在超寬帶無線網絡的協同路由算法，用以降低原先路由在衰落和多用戶干擾環境下的中斷概率。首先，我們需要設定一條單路徑(single path)路由。然後，協同路由算法便決定有沒有其他「偷聽」到之前一跳訊息的節點，可以與原先應該在這跳傳送的節點作協同傳輸。結果顯示我們的協同路由算法能夠節省平均傳送能量而達到特定的中斷概率。

Abstract of thesis entitled:

Cooperative Routing in Wireless Ad Hoc Networks

Submitted by CHEUNG, Man Hon

for the degree of Master of Philosophy

at The Chinese University of Hong Kong in June 2007

In a wireless ad hoc network, the prime design challenge is the limited supply of energy. In this work, we consider energy-efficient routing based on two physical layer models: binary digital transmission in Rayleigh fading channel and Pulse Position Modulation - Time Hopping - Ultra-Wideband (PPM-TH-UWB) system. Cooperative routing and interference-aware routing algorithms using these models are studied.

In the first part of our work, we consider cooperative routing in Rayleigh fading channel. Two nodes are involved in cooperative communications in each hop. They are placed at different distances to the single receiver in general and the total transmit power for each hop is constant. We determine criteria for cooperation and transmit power distribution between the two nodes in case of cooperation in order to reduce the probability of outage, which is defined to be the probability that the receive signal-to-noise ratio (SNR) per bit is smaller than a certain threshold Θ. We perform analyses and simulations on outage performance of cooperative and non-cooperative schemes in a 1D Poisson random network and a 2D grid network. Furthermore, we suggest a cooperative routing algorithm and evaluate its outage performance in 2D random networks. From our results, the cooperative schemes achieve a diversity order of two.

Next, we study interference-aware and cooperative routing using UWB physical layer model. We first derive the Bit Error Rate (BER) performance for PPM-TH-UWB systems under Additive White Gaussian Noise (AWGN) and Multi-User Interference (MUI) using Rake receiver, based on the work of [48], [12] and [5].

Based on the above results, interference-aware routing in UWB wireless networks is suggested. It aims to find route which has the minimum transmit energy per bit, given the positions of the source, destination and BER requirement. We first derive a suitable link cost based on the BER expression derived. With this link cost, we introduce an Optimal Interference-Aware Routing Algorithm, which is capable of routing data packets from source to destination, using minimum energy per bit and at the same time achieving the end-to-end BER requirement. A Simple Interference-Aware Routing Algorithm with a lower complexity is also introduced. From our result, it is shown that our Interference-Aware routing Algorithms consume less energy than some simple routing algorithms.

Then, cooperative routing in UWB wireless networks is studied. It aims to reduce the energy consumption of a single path route, given the outage performance requirement. The effect of both fading and MUI is considered. The setup in this part is similar to that in the first part of the thesis, except with the presence of other UWB interferers. We first generate a single path route from any available routing algorithms. Based on this single path route, our Cooperative Routing Algorithm is executed to see whether nodes which "overhear" the information should cooperate to alleviate the effect of fading, and thus improves outage performance. From our result, it is shown that our Cooperative Routing Algorithm reduces the average transmit energy in order to achieve a certain outage performance in a given grid network.

Acknowledgement

"Who are they that fear the LORD? He will teach them the way that they should choose."(Psalms 25:12)

First and foremost, I would like to thank my LORD for accompanying me in every stage of my life and guiding me in my research. Without his grace, I would have achieved nothing.

I wish to express my deep gratitude to my supervisor, Prof. Tat Ming LOK for his expert supervision and willingness to meet me in his busy schedule. Besides teaching me a lot about wireless communications, he shared with me a lot of useful strategies in "playing the game of research".

I wish to record my gratitude to my dad, mom and sister for their love and support in my life. The road of research would be a lot tougher and lonely without their care.

I also hope to thank my brothers and sisters in Luke Fellowship in my church. I am grateful to their sharing and prayers which encourage me to work hard in following the steps of our Almighty LORD.

This work is dedicated to my LORD and my family.

Contents

List of Figures

Chapter 1

Introduction

In this thesis, we study cooperative routing based on two physical layer models, namely PPM-TH-UWB wireless systems and simple binary digital transmission in Rayleigh fading channels. Moreover, interference-aware routing in PPM-TH-UWB wireless systems is considered. We aim to find routing and transmission strategies that reduce the energy consumption given a certain performance requirement or improve the performance criteria given an energy constraint.

In this chapter, we go through three important communication concepts and techniques in this thesis, namely Rayleigh fading channels, UWB communications and cooperative communications.

1.1 Rayleigh Fading Channels

When modeling a wireless channel, besides the thermal noise at the receiver front end, the effects of path loss, shadowing and multipath fading need to be considered.

Path loss refers to the dissipation of transmit signal power which results from the propagation of the electromagnetic wave over a distance. Shadowing is the attenuation of the signal power due to the presence of fixed obstacles in the transmission path. Both path loss and shadowing are grouped under large-scale fading that represents the average attenuation of signal power due to motion over large areas [44].

Moreover, signal travels in a multipath fashion, which it takes on multiple paths to the receiver after encountering the effects of reflection, scattering and diffraction. As a result, the amplitude, phase and angle of arrival of the signal fluctuate. This phenomenon is called multipath fading. It is grouped under small-scale fading that represents the dynamic changes in amplitude and phase due to small variation in distance between transmitter and receiver [44].

Additionally, when the number of multipath component is large and that there is no Line-of-Sight (LOS) multipath component between the transmitter and receiver, the envelope of the received signal can be modeled by a Rayleigh distribution, which is given by

$$p(r) = \begin{cases} \frac{r}{\sigma^2} \exp\left(-\frac{r^2}{2\sigma^2}\right) & \text{for } r \geq 0 \\ 0 & \text{otherwise} \end{cases} \tag{1.1}$$

where r is the amplitude of the envelope of the received signal and $2\sigma^2$ is the pre-detection mean power of the multipath signal [44].

1.2 Ultra-Wideband (UWB) Communications

1.2.1 Definition

Generally speaking, Ultra-Wideband (UWB) communication refers to the radiation of signal which has an instantaneous bandwidth many times greater than the minimum required bandwidth to deliver the information [35].

To understand the more precise definition of UWB, we need to know how bandwidth is defined by the Federal Communications Commission (FCC) in US. We define f_L and f_H to be the lower and upper -10dB emission points at the energy spectrum respectively as shown in Fig. 1.1. The Energy Bandwidth (EB) is defined to be the difference between f_L and f_H and is given by $EB = f_H - f_L$. Central frequency (f_c) of the spectrum is defined to be the average of f_L and f_H and is given by $f_C = 0.5(f_H + f_L)$. Fractional Bandwidth (FB) is defined to be the ratio of EB

to f_C: $FB = EB/f_C = 2(f_H - f_L)/(f_H + f_L)$.

According to the FCC, the definition of UWB is different below and above the threshold central frequency f_C of 2.5GHz. If $f_C < 2.5GHz$, a signal is regarded as UWB if its FB is larger than 0.20. If $f_C > 2.5GHz$, a signal is regarded as UWB if its EB is larger than 500MHz.

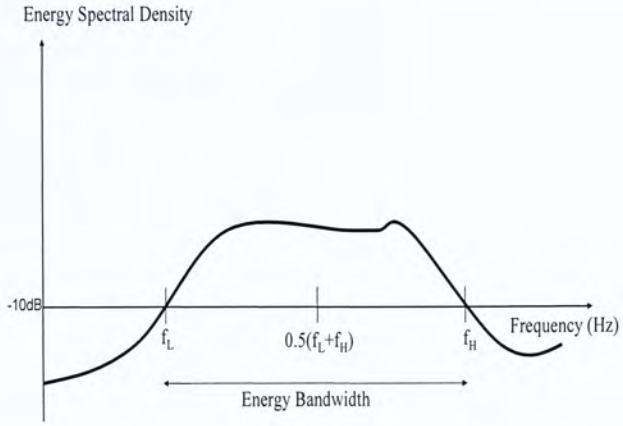

Figure 1.1: Energy Spectrum.

1.2.2 Characteristics

UWB has a lot of nice features ([35] and [4]) which are different from traditional narrowband system:

1. Large Instantaneous Bandwidth

   The most obvious feature of UWB is its huge instantaneous bandwidth. High data rate indoor application of above 110Mbps can be supported.

2. Low Power Spectral Density

   Due to the low power spectral density and the pseudo-random characteristics of

UWB signal, the probability of detection or interception of UWB signal by unintended users is very low, which makes it an excellent choice for secure or military applications. Moreover, because of its low-power and noise-like transmission, UWB can overlay with already available services, such as Global Positioning System (GPS) and Wireless Local Area Networks (WLANs), without causing significant interference.

3. Low Complexity and Low Cost

   Unlike conventional wireless communication systems, UWB transmitters send pulses of short duration without the need of modulation by a carrier frequency. Without the local oscillator, complex delay and phase lock loops at the receivers for baseband transmission, the complexity and cost are greatly reduced.

4. Multipath Immunity

   Because of the use of short pulses, a number of resolvable paths can be exploited at the receiver end in a dense multipath environment. Robustness and performance can be improved significantly by this form of multipath diversity.

5. Fine Time-Domain Resolution

   Because of the very narrow pulses generated by UWB radios, UWB can offer better timing precision than GPS. Together with good material penetration properties, UWB can readily support short-range radar applications, such as surveying, mining and rescue.

1.2.3 UWB Signals

UWB signals are commonly generated by two methods. The traditional way is to radiate pulses of very short duration, typically in the order of nanosecond. This kind of UWB is called Impulse Radio-UWB (IR-UWB). In IR-UWB, pulses can be modulated by techniques like Pulse Position Modulation (PPM) or Pulse Amplitude Modulation (PAM). Moreover, in order to allow multiple access, spread spectrum

techniques such as Time Hopping (TH) or Direct Sequence (DS) are also employed. Another way to generate UWB signal is to use multiple simultaneous carriers to convey information at high data rate. This form of UWB is named as Multicarrier-UWB (MC-UWB). In this thesis, we use PPM-TH-UWB, a form of IR-UWB, as the signaling format.

There are some pros and cons for IR-UWB and MC-UWB. For IR-UWB, it is cheap and simple because only baseband transmission is employed. However, high precision in synchronization is required for its proper operation. For MC-UWB, it can provide a high data rate transmission and is capable of avoiding interference because its carrier frequency can be chosen accordingly to avoid narrowband interference. However, it comes at a cost of higher hardware complexity.

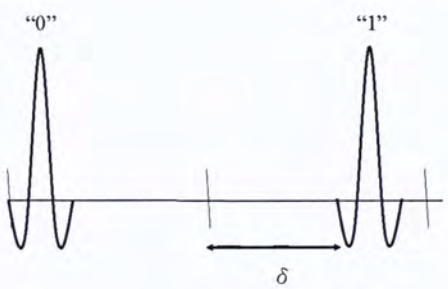

Figure 1.2: Pulse Position Modulation: the positions for the left and right pulses are used to convey information for bits "0" and "1" respectively. δ is used to denote the difference in position that the "1" pulse needed to move with respect to the reference position, which is the position of "0" pulse in this case.

1.2.4 Applications

UWB is an excellent candidate to support a number of new wireless applications. Some of them are discussed below:

- Short-Range, High Data Rate Wireless Personal Area Networks (WPANs):
  The IEEE has established the 802.15.3a physical layer standard for short range

and high data rate applications. The minimum data rate expected is 110Mbps at a transmission distance of 10m. UWB can be used in WPANs to address short-range ad-hoc connectivity among consumer electronic and communication devices. Potential applications include high-quality real-time video and audio distribution, file exchange among storage systems, and cable replacement for home entertainment systems. [51]

- Low-Rate WPANs:
  The IEEE has defined another standard of 802.15.4 for low data rate, low power and low complexity applications. Potential applications include sensors, home automation and remote controls that power consumption should be kept as small as possible.

- Sensor Networks:
  Sensor networks consist of a large number of nodes deployed over a region. They are used to monitor changes in environment. Because of the nature of sensing devices and difficulty in recharging their batteries, limited power supply is a much serious problem for sensor network than WPANs.

- Imaging Systems:
  UWB radar pulses are always shorter than the dimension of the target. They reflect from target not only with changes in amplitude and time shift, but also with changes in pulse shape. As a result, UWB has shown a better sensitivity than traditional radar systems. Typical applications include ground-penetrating radars, medical diagnosis and ocean imaging.

For a more comprehensive introduction to UWB, interesting readers can refer to the work of [51], [52] and [33].

1.3 Cooperative Communications

In wireless communication, because of the effect of multipath fading, the channels are sometimes good and sometimes bad. Occasionally, if the user experiences a very bad channel, the performance is severely affected. A solution to this problem is cooperative diversity. Because of the broadcast nature of wireless communication, all users around the sender should be able to receive a copy of the signal. They can act as relays and provide the receiver with extra copies of the transmitted signal through independent channels. In this way, channels are averaged out, variations are reduced and performance of transmission is more stable.

We consider the network as shown in Fig. 1.3, in which node S intends to send information to node T. In wireless communication, because of the effect of multipath fading, the channels are sometimes good and sometimes bad. Occasionally, if the signal from node S to node T experiences a very bad channel, node T will receive a poor copy of the signal and the performance will be severely affected.

One solution to this problem is cooperative diversity. Because of the broadcast nature of wireless communication, node R "overhears" a copy of the signal intended to node T. As the fading channels between nodes S and T and that between nodes R and T are independent, node R can act as relay and provides node T with an extra copy of the transmitted signal through the independent channel between R and T. Since Node T receives two copies of the signals through two independent channels, the chance that the two channels are bad simultaneously is low. As a result, the effect of channel variation is averaged out and the performance of transmission is more stable.

1.4 Outline of Thesis

The rest of the thesis is organized as follows: chapter 2 reviews the literature on topics including interference-aware routing, link cost, routing in UWB wireless network,

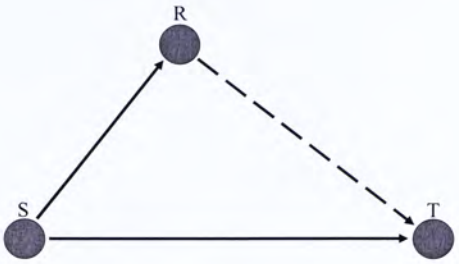

Figure 1.3: Cooperative communication.

cooperative communications and cooperative routing. In chapter 3, two-node cooperative routing in Rayleigh fading channel is presented. Chapter 4 describes the UWB system model and derives the BER expression. The use of rake receivers is discussed and some simple routing algorithms in 1D network are compared. Interference-aware routing and cooperative routing in UWB wireless networks are discussed in chapters 5 and 6 respectively. Conclusions and future extension of the research are given in chapter 7.

Chapter 2

Background Study

In this chapter, we will review some previous work about interference-aware routing, link cost and the routing issues that have been addressed in UWB wireless networks. Next, we will study the recent advancement of cooperative communications and the incorporation of the idea of cooperative communications into the context of routing.

2.1 Interference-Aware Routing

A wireless ad hoc network is a collection of mobile hosts that form a temporary network to communicate with each other without the aid of any centralized control and established infrastructures. When some of the nodes are transmitting at the same time, they may cause interference to the others. We called this phenomenon Multi-User Interference (MUI).

There has been some work on interference-based routing. In [19], a multihop routing algorithm named Balanced Interference Routing Algorithm (BIRA) is introduced. It takes into the effect of MUI by incorporating it into the link cost. Specifically, the link cost is the linear combination of a fixed cost and interference level. The link cost between node i and j is

$$C_{ij} = \beta A_{ij} + (1 - \beta) I L_{ij} \tag{2.1}$$

where β is the weight factor with value between 0 and 1. A_{ij} is the fixed cost and is taken to be 1 in its performance evaluation. For a interfered node r, the interference it receive from link ij is the sum of the transmission power from node i to node j and that from node j to node i. IL_{ij} is interference level of the link ij generated to other interfered nodes in the network and is given by

$$IL_{ij} = \sum_{r \neq i, r \neq j} \left(\left(\frac{D_{ij}}{D_{ir}} \right)^{\alpha} + \left(\frac{D_{ji}}{D_{jr}} \right)^{\alpha} \right) \tag{2.2}$$

where D_{ab} is the Euclidean distance between nodes a and b. α is the path loss exponent. By using the link cost C_{ij} and applying Dijkstra's Algorithm, a route that causes the minimum amount of interference to other nodes in the network is obtained.

Routing algorithm that aims to minimize total energy consumption in multihop wireless network is proposed in [23]. It is a cross-layer design which takes into the account the effect of interference (physical layer) caused by existing flows and power control (MAC layer). An interference-aware QoS routing algorithm that guarantees bandwidth requirement in realistic interference environment is proposed in [7]. Multiple paths are discovered but only the best one is selected. In [15], a heuristic interference-aware QoS routing algorithm is suggested. It is primarily based on local knowledge and state information at the source node. Interference-aware routing in multihop wireless networks using directional antennae with dynamic traffic is studied in [46]. It should be noted that the term "interference" of a link discussed in [15] and [46] refers to the amount of traffic that goes through the link at the link layer, but not the signal interference at the physical layer.

Some other works in interference-based routing include the Least Interference Routing in [37]. There are also some works on Minimum Interference Routing ([22] and [13]). However, they are related to Multi-Protocol Label Switched (MPLS) networks, which are not wireless. The work "interference" does not mean the MUI at the physical layer, but the networking load occupied by other users.

2.2 Routing in UWB Wireless Networks

In [28] and [29], power-efficient routing in UWB mobile networks is considered. The link cost c is the sum of both the signaling cost and transmission cost

$$c = \delta C_0 d^\alpha + C_1 R d^\alpha \tag{2.3}$$

The first part of the summation is the signaling cost. If there is an active link between the two nodes, no signaling cost is required and so $\delta = 0$. Otherwise, a signaling cost is required and $\delta = 1$. C_0 and C_1 are constants used to weigh the signaling and transmission cost. R is the data rate and d is the distance between the two nodes in the link. α is the path loss exponent. Though MUI is not included in the link cost, it has been taken account in the interference model of its performance evaluation.

In [2], the cost function is improved further to consider more parameters in the route selection which the cost function for each link is of the form

$$C(x,y) = C(power)+C(sync)+C(interference)+C(quality)+C(delay)+C(other) \tag{2.4}$$

where the $C(power)$ and $C(sync)$ are related to power and synchronization and are similar to the two terms in (2.3). $C(interference)$ is related to the interference. $C(quality)$ is about the quality or reliability of a link. $C(delay)$ is related to the delay in communication caused by each hop in the potential route. $C(other)$ is included so that the cost function can be tailored to a specific type of network, such as voice networks, data networks and sensor networks, etc.

Energy-aware and link adaptive routing for UWB wireless sensor networks is considered in [50]. It is energy-aware in that it takes care of the next-hop remaining battery capacity in its routing metric. Also, it is link adaptive because it uses adaptive modulation that changes its modulation method with respect to the link condition.

Some location-aware routing algorithms are suggested which make use of the high precision localization capability of UWB. With the use of location information, nodes

can choose to send packets to neighbours which are closer to the destinations [20]. In [1], a position-based quality-of-service (QoS) routing scheme for UWB wireless networks is suggested. It takes care of the interactions in Medium Access Control (MAC) layer and applies call admission control and temporary bandwidth reservation for discovered routes. The QoS includes packet loss, delay and throughput performance guarantee.

Moreover, routing, power control and scheduling in UWB networks have been formulated as a joint optimization problem in [34]. Its objective is to maximize flow rates given node power constraints. The work in [49] tries to optimize the network throughput by considering both routing and network topology formation and formulating it as a nonlinear programming problem.

2.3 Cooperative Communications and Routing

In a wireless channel, the transmitted signal from the sender can take multiple paths to reach the receivers. The different copies of the signal normally arrive at the receiver with different amplitudes and phases. Due to the constructive and destructive interference of multiple signal components which are randomly delayed, reflected, scattered and diffracted, signal attenuation may vary significantly during the transmission process. This phenomenon is called multipath fading [43].

Cooperative communication is proposed to combat the multipath fading by providing transmit diversity [30]. It takes advantage of the multipath propagation of the signal and provides the receiver with different replicas of the transmitted signal. If these copies undergo independent fading, the chance that all of them experience deep fading simultaneously is small. However, the transmit diversity is obtained by sharing the use of antennae among users, instead of having multiple antennae for each user.

In [39], [40] and [41], user cooperative strategies, implementation issues and performance analysis in a cellular environment are discussed. It has shown that when

cooperative communication is used, capacity is increased and rates of users are less susceptible to channel variations due to fading.

Low-complexity cooperative diversity protocols are developed in [25] and [24]. The protocols include fixed relaying schemes (e.g. amplify-and-forward and decode-and-forward), selection relaying schemes that are adaptive version of fixed relaying schemes and incremental relaying schemes that perform adaptation based on the limited feedback from the destination terminal. Outage probability of theses schemes are analyzed.

Physical layer of multihop wireless channels is analyzed in [6]. Four channel models for multihop transmission, namely amplified, decoded, amplified diversity and decoded diversity relaying multihop channels, are studied. Reception probability and power distribution in selection combining diversity schemes have been analyzed in [17] using "erristor approach". Two-phase cooperative communication with space-time coding in Poisson wireless networks is studied in [45], which source node broadcasts information to relay nodes in phase I and relay nodes cooperatively transmit to sink node using space-time coded packets in phase II.

The work in [36] tries to bridge the gap between physical layer and higher layer research in cooperative communications. Possible architectures in cooperative networks are discussed to provide modified wireless link abstractions. Considering cooperation in the context of routing, the work in [21] has considered the joint problem of transmit diversity and routing. It has shown that cooperative routing consumes less energy than non-cooperative routing, by taking the assumption that senders can adjust the phases of transmitted signals to allow them to arrive in phase at the receivers. Power-optimal cooperative routing and power distribution strategies in fading channels using spread spectrum system are studied in [9]. The effects of cooperative diversity, multihopping and power distribution among cooperating links are studied. The work in [14] considers a multihop network with multiple relays at each hop. Three cooperative routing strategies are proposed to achieve full diversity

gain and minimize the end-to-end outage from the link layer point of view. Cooperation among relay nodes is in the form of choosing a good (or best) link for each hop.

□ **End of chapter.**

Chapter 3

Cooperative Routing in Rayleigh Fading Channel

In this chapter, we consider cooperative routing in Rayleigh fading channel. For each hop, two nodes are involved in cooperative communications. The two nodes are placed at different distances to the single receiver in general and the total transmit power for each hop is constant. We determine criteria for cooperation and transmit power distribution between the two nodes in case of cooperation in order to reduce the probability of outage, which is defined to be the probability that the receive signal-to-noise ratio (SNR) per bit is smaller than a certain threshold Θ. We perform analyses and simulations on outage performance of cooperative and non-cooperative schemes in a 1D Poisson random network and a 2D grid network. Furthermore, we suggest a cooperative routing algorithm and evaluate the outage performance of the routes in 2D random networks.

3.1 System Model

3.1.1 Transmitted Signal

Consider that source S is going to send packets to sink T. As shown in Fig. 3.1, node 1 is used as the relay and we assume that node 1 has received the message correctly from S. Because of the broadcast nature of wireless communication, node 2 also receives the signal from S to node 1. As a result, node 2 can cooperate with node 1 and send to node T at the same time. We assume that transmit power for nodes 1 and 2 are βP and $(1-\beta)P$ respectively, where $0 \leq \beta \leq 1$. That means the total transmit power to node T is P, but it is distributed between nodes 1 and 2 according to a certain ratio β. The transmitted signal for nodes 1 and 2 are

$$\begin{aligned} s_1(t) &= b\sqrt{\beta P}c_1(t) \\ s_2(t) &= b\sqrt{(1-\beta)P}c_2(t), t \in [0,T] \end{aligned} \tag{3.1}$$

where $b \in \{-1, 1\}$ is the data bit. $c_i(t)$ is the direct-sequence spreading waveform used by node i for communication in a multi-user environment [9] and we assume that the spreading waveform has a low spreading gain. T is the symbol duration. Non-cooperative transmissions are the cases when $\beta = 0$ or 1, and two-node cooperative transmissions are the cases when $0 < \beta < 1$.

3.1.2 Received Signal and Maximal-Ratio Combining (MRC)

We assume that the wireless channel experiences frequency non-selective Rayleigh fading, which is a valid assumption in our spread spectrum system due to the low spreading gain waveform that we choose. The channel for node i is given by $h_i(t) = \frac{h_i}{\sqrt{d_i^\alpha}}\delta(t-\tau_i)$, where h_i is a Rayleigh distributed random variable with variance σ^2 and we assume that $2\sigma^2 = 1$. τ_i is the delay of the received signal at node T from node i. d_i is the distance between node i and the receiver T. α is the path loss exponent. The received signal is thus of the form

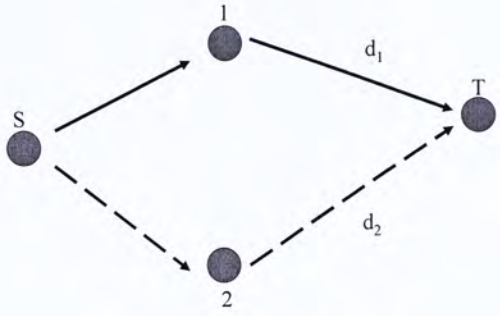

Figure 3.1: Non-Cooperative ($S \rightarrow 1 \rightarrow T$) vs. Cooperative Routing ($S \rightarrow \{1,2\} \rightarrow T$).

$$\begin{aligned} r(t) &= s_1(t) * h_1(t) + s_2(t) * h_2(t) + n(t) \\ &= \frac{h_1}{\sqrt{d_1^\alpha}} s_1(t-\tau_1) + \frac{h_2}{\sqrt{d_2^\alpha}} s_2(t-\tau_2) + n(t) \\ &= b\sqrt{\frac{\beta P}{d_1^\alpha}} h_1 c_1(t-\tau_1) + b\sqrt{\frac{(1-\beta)P}{d_2^\alpha}} h_2 c_2(t-\tau_2) + n(t), t \in [0,T] \end{aligned} \tag{3.2}$$

where $n(t)$ is a zero mean, additive white Gaussian noise (AWGN) random process with two-sided power spectral density $N_0/2$. Assume that the orthogonal codes are orthogonal such that $\int_0^T c_1(t-\tau_1)c_2(t-\tau_2)dt = 0$ and that they are normalized such that $\int_0^T c_i^2(t-\tau_i)dt = 1$ for $i = 1$ or 2.

The decision variables for the reception of the signals $s_1(t)$ and $s_2(t)$ are

$$y_1 = \int_0^T r(t)c_1(t-\tau_1)dt = b\sqrt{\frac{\beta P}{d_1^\alpha}} h_1 + n_1 = A_1 h_1 + n_1 \tag{3.3}$$

$$y_2 = \int_0^T r(t)c_2(t-\tau_2)dt = b\sqrt{\frac{(1-\beta)P}{d_2^\alpha}} h_2 + n_2 = A_2 h_2 + n_2 \tag{3.4}$$

where $A_1 = b\sqrt{\frac{\beta P}{d_1^{\alpha}}}$, $A_2 = b\sqrt{\frac{(1-\beta)P}{d_2^{\alpha}}}$, $n_1 = \int_0^T n(t)c_1(t-\tau_1)dt$ and $n_2 = \int_0^T n(t)c_2(t-\tau_2)dt$.

Using MRC, the decision variable for detection is

$$\begin{aligned} Z &= A_1 h_1 y_1 + A_2 h_2 y_2 \\ &= (A_1^2 h_1^2 + A_2^2 h_2^2) + (A_1 h_1 n_1 + A_2 h_2 n_2) \end{aligned} \tag{3.5}$$

with

$$E[Z] = A_1^2 h_1^2 + A_2^2 h_2^2 \tag{3.6}$$

$$\begin{aligned} Var[Z] &= A_1^2 h_1^2 Var[n_1] + A_2^2 h_2^2 Var[n_2] \\ &= (A_1^2 h_1^2 + A_2^2 h_2^2)\frac{N_0}{2} \end{aligned} \tag{3.7}$$

Output signal-to-noise ratio (SNR) from the receiver is equal to

$$\frac{E[Z]^2}{Var[Z]} = 2\left(\frac{\beta P d_1^{-\alpha}}{N_0} h_1^2 + \frac{(1-\beta)P d_2^{-\alpha}}{N_0} h_2^2\right) = 2\gamma_b \tag{3.8}$$

where

$$\gamma_b = \frac{\beta P d_1^{-\alpha}}{N_0} h_1^2 + \frac{(1-\beta)P d_2^{-\alpha}}{N_0} h_2^2 \tag{3.9}$$

is the SNR per bit.

3.1.3 Probability of Outage

We define probability of outage to be the probability that the SNR per bit of the received signal is smaller than a certain threshold Θ, i.e.

$$p_{out} = P(\gamma_b < \Theta) \tag{3.10}$$

As a result for non-cooperative transmission with $\beta = 1$

$$p_{out,1} = P(\frac{P d_1^{-\alpha}}{N_0} h_1^2 < \Theta) = P(h_1 < \sqrt{\frac{\Theta N_0}{P d_1^{-\alpha}}}) = 1 - \exp\left(-\frac{\Theta N_0}{P d_1^{-\alpha}}\right) \tag{3.11}$$

because h_1 is a Rayleigh random variable with variance $\sigma^2 = 1/2$. Similarly, for $\beta = 0$, we have

$$p_{out,2} = P(\frac{P d_2^{-\alpha}}{N_0} h_2^2 < \Theta) = 1 - \exp\left(-\frac{\Theta N_0}{P d_2^{-\alpha}}\right) \tag{3.12}$$

For cooperative case when $0 < \beta < 1$, we notice that γ_b in (3.9) is the sum of two independent central chi-square random variables ([42] and [32]), each with two degrees of freedom.

Let $Y = X_1^2 + X_2^2$, where $X_1 \sim \text{Rayleigh}(\sigma_1^2)$ and $X_2 \sim \text{Rayleigh}(\sigma_2^2)$. As mentioned in [42], for the case that $\sigma_1 \neq \sigma_2$, Y is the sum of two independent central chi-square distributions with parameters equal to σ_1^2 and σ_2^2 respectively and each with two degrees of freedom. The probability density function (pdf) $p_Y(y)$ and cumulative distribution function (cdf) $F_Y(y)$ of Y for $y \geq 0$ are given by

$$p_Y(y) = \frac{1}{2(\sigma_2^2 - \sigma_1^2)} \left(\exp\left(-\frac{y}{2\sigma_2^2}\right) - \exp\left(-\frac{y}{2\sigma_1^2}\right) \right) \tag{3.13}$$

$$F_Y(y) = 1 - \left(\frac{\sigma_2^2}{\sigma_2^2 - \sigma_1^2}\right) \exp\left(-\frac{y}{2\sigma_2^2}\right) + \left(\frac{\sigma_1^2}{\sigma_2^2 - \sigma_1^2}\right) \exp\left(-\frac{y}{2\sigma_1^2}\right) \tag{3.14}$$

For the case which $\sigma_1 = \sigma_2 = \sigma$, Y is a central chi-square distribution with $n = 2m = 4$ degrees of freedom (so $m = 2$) [32]. The pdf and cdf of Y for $y \geq 0$ are given by

$$p_Y(y) = \frac{1}{2\sigma^2 \Gamma(m)} \left(\frac{y}{2\sigma^2}\right)^{m-1} \exp\left(-\frac{y}{2\sigma^2}\right) = \frac{1}{2\sigma^2} \left(\frac{y}{2\sigma^2}\right) \exp\left(-\frac{y}{2\sigma^2}\right) \tag{3.15}$$

$$F_Y(y) = 1 - \exp\left(-\frac{y}{2\sigma^2}\right) \sum_{i=0}^{m-1} \frac{1}{i!} \left(\frac{y}{2\sigma^2}\right)^i = 1 - \exp\left(-\frac{y}{2\sigma^2}\right) \left(1 + \frac{y}{2\sigma^2}\right) \tag{3.16}$$

We first consider $p_{out,3}$ for $\beta \neq \frac{d_1^\alpha}{d_1^\alpha + d_2^\alpha}$. For this case, we have

$$\begin{aligned} p_{out,3} &= P(\gamma_b = \tfrac{\beta P d_1^{-\alpha}}{N_0} h_1^2 + \tfrac{(1-\beta) P d_2^{-\alpha}}{N_0} h_2^2 < \Theta) \\ &= P(X_1^2 + X_2^2 < \Theta) \\ &= F_Y(\Theta) \\ &= 1 - \tfrac{(1-\beta) d_1^\alpha}{(1-\beta) d_1^\alpha - \beta d_2^\alpha} \exp\left(-\tfrac{\Theta N_0 d_2^\alpha}{(1-\beta) P}\right) + \tfrac{\beta d_2^\alpha}{(1-\beta) d_1^\alpha - \beta d_2^\alpha} \exp\left(-\tfrac{\Theta N_0 d_1^\alpha}{\beta P}\right) \end{aligned} \tag{3.17}$$

where $X_1^2 = \frac{\beta P d_1^{-\alpha}}{N_0} h_1^2$, $X_2^2 = \frac{(1-\beta) P d_2^{-\alpha}}{N_0} h_2^2$ and $Y = X_1^2 + X_2^2$. Assume that h_1, $h_2 \sim$ Rayleigh(σ^2) and $2\sigma^2 = 1$, we have $X_1 \sim$ Rayleigh($\sigma_1^2 = \frac{\beta P d_1^{-\alpha}}{N_0}\sigma^2$) and $X_2 \sim$ Rayleigh($\sigma_2^2 = \frac{(1-\beta) P d_2^{-\alpha}}{N_0}\sigma^2$). Substituting $y = \Theta$, $\sigma_1^2 = \frac{\beta P d_1^{-\alpha}}{N_0}\sigma^2$ and $\sigma_2^2 = \frac{(1-\beta) P d_2^{-\alpha}}{N_0}\sigma^2$ into (3.14), we obtain the last line of the above equation.

Next, we first consider $p_{out,3}$ for $\beta = \frac{d_1^\alpha}{d_1^\alpha + d_2^\alpha}$. For this case, we have

$$\begin{aligned} p_{out,3} &= P(\gamma_b = \tfrac{\beta P d_1^{-\alpha}}{N_0} h_1^2 + \tfrac{(1-\beta) P d_2^{-\alpha}}{N_0} h_2^2 < \Theta) \\ &= P(h_1^2 + h_2^2 < \tfrac{\Theta N_0 (d_1^\alpha + d_2^\alpha)}{P}) \\ &= F_Y(\tfrac{\Theta N_0 (d_1^\alpha + d_2^\alpha)}{P}) \\ &= 1 - \exp\left(-\tfrac{\Theta N_0 (d_1^\alpha + d_2^\alpha)}{P}\right)\left(1 + \tfrac{\Theta N_0 (d_1^\alpha + d_2^\alpha)}{P}\right) \end{aligned} \tag{3.18}$$

where $Y = h_1^2 + h_2^2$, with h_1, $h_2 \sim$ Rayleigh(σ^2) and $2\sigma^2 = 1$. Substituting $y = \frac{\Theta N_0 (d_1^\alpha + d_2^\alpha)}{P}$ and $2\sigma^2 = 1$ into (3.16), we obtain the last line of the above equation.

In conclusion, the probability of outage for cooperation is given by

$$p_{out,3} = \begin{cases} 1 - \exp\left(-\frac{\Theta N_0 (d_1^\alpha + d_2^\alpha)}{P}\right)\left(1 + \frac{\Theta N_0 (d_1^\alpha + d_2^\alpha)}{P}\right) & \text{for } \beta = \frac{d_1^\alpha}{d_1^\alpha + d_2^\alpha} \\ 1 - \frac{(1-\beta) d_1^\alpha}{(1-\beta) d_1^\alpha - \beta d_2^\alpha} \exp\left(-\frac{\Theta N_0 d_2^\alpha}{(1-\beta) P}\right) + \frac{\beta d_2^\alpha}{(1-\beta) d_1^\alpha - \beta d_2^\alpha} \exp\left(-\frac{\Theta N_0 d_1^\alpha}{\beta P}\right) & \text{otherwise} \end{cases} \tag{3.19}$$

Moreover, $p_{out,3}$ is continuous for $\beta \in [0, 1]$. It is obvious that $p_{out,3}$ is continuous for all the points where $\beta \in [0, 1]$, except for the point $\beta = \frac{d_1^\alpha}{d_1^\alpha + d_2^\alpha}$ which requires more careful consideration. Because

$$
\begin{aligned}
&\lim_{\beta \to \frac{d_1^\alpha}{d_1^\alpha + d_2^\alpha}} 1 - \frac{(1-\beta)d_1^\alpha}{(1-\beta)d_1^\alpha - \beta d_2^\alpha} \exp\left(-\frac{\Theta N_0 d_2^\alpha}{(1-\beta)P}\right) + \frac{\beta d_2^\alpha}{(1-\beta)d_1^\alpha - \beta d_2^\alpha} \exp\left(-\frac{\Theta N_0 d_1^\alpha}{\beta P}\right) \\
&= 1 - \lim_{\beta \to \frac{d_1^\alpha}{d_1^\alpha + d_2^\alpha}} \frac{(1-\beta)d_1^\alpha \exp\left(-\frac{kd_2^\alpha}{(1-\beta)}\right) - \beta d_2^\alpha \exp\left(-\frac{kd_1^\alpha}{\beta}\right)}{(1-\beta)d_1^\alpha - \beta d_2^\alpha} \\
&= 1 - \lim_{\beta \to \frac{d_1^\alpha}{d_1^\alpha + d_2^\alpha}} \frac{d_1^\alpha \exp\left(-\frac{kd_2^\alpha}{(1-\beta)}\right)\left(-\frac{kd_2^\alpha}{1-\beta} - 1\right) - d_2^\alpha \exp\left(-\frac{kd_1^\alpha}{\beta}\right)\left(1 + \frac{kd_1^\alpha}{\beta}\right)}{-d_1^\alpha - d_2^\alpha} \\
&= 1 - \exp[-k(d_1^\alpha + d_2^\alpha)][1 + k(d_1^\alpha + d_2^\alpha)] \\
&= 1 - \exp\left(-\frac{\Theta N_0 (d_1^\alpha + d_2^\alpha)}{P}\right)\left(1 + \frac{\Theta N_0 (d_1^\alpha + d_2^\alpha)}{P}\right)
\end{aligned}
\tag{3.20}
$$

where $k = \frac{\Theta N_0}{P}$. So, $p_{out,3}$ is also continuous at $\beta = \frac{d_1^\alpha}{d_1^\alpha + d_2^\alpha}$. The 3rd line is obtained by applying L'Hospital's Rule to $\frac{0}{0}$ form.

3.2 Cooperation Criteria and Power Distribution

3.2.1 Optimal Power Distribution Ratio

We are interested to find the optimal β that minimizes $p_{out,3}$. This can be done numerically with low complexity by searching for the minimum value of $p_{out,3}$ in the range $0 \leq \beta \leq 1$. Typical graphs of $p_{out,1}$, $p_{out,2}$ and $p_{out,3}$ vs. β are shown in Fig. 3.2. As seen in this figure, the portion of β which $p_{out,3}$ is less than $p_{out,1}$ and $p_{out,2}$ is the power distribution ratio which cooperation is desirable.

3.2.2 Near-Optimal Power Distribution Ratio β'

Though the optimal power distribution ratio β can be obtained with low complexity, its close form solution is hard to obtain. So we propose a near-optimal power distribution ratio β' which is given by

$$
\beta' = \frac{\exp\left(-\frac{\Theta N_0}{P d_1^{-\alpha}}\right)}{\exp\left(-\frac{\Theta N_0}{P d_1^{-\alpha}}\right) + \exp\left(-\frac{\Theta N_0}{P d_2^{-\alpha}}\right)} = \frac{\exp(k d_2^\alpha)}{\exp(k d_1^\alpha) + \exp(k d_2^\alpha)} \tag{3.21}
$$

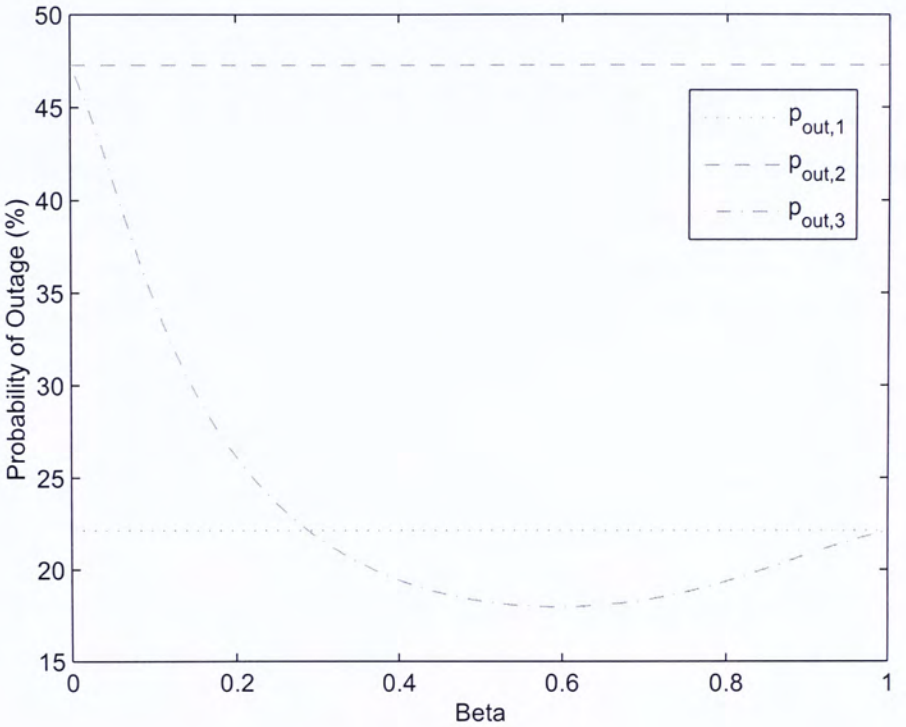

Figure 3.2: $p_{out,1}$, $p_{out,2}$ and $p_{out,3}$ vs. β for $d_1 = 5$, $d_2 = 8$, transmit SNR = 20dB.

where $k = \frac{\Theta N_0}{P}$. $\exp\left(-\frac{\Theta N_0}{P d_i^{-\alpha}}\right)$ is the reception probability when the transmission distance is d_i with P being the transmit power. It has been shown by our experiment that β' is close to the optimal β when $\frac{P d_1^{-\alpha}}{N_0} > \Theta$ AND $\frac{P d_2^{-\alpha}}{N_0} > \Theta$. Moreover, we observe some insightful properties for β'. When transmit power P is large, the system is insensitive to the power distribution between the two channels, so β' is close to 0.5. When $d_2 >> d_1$, transmission through distance d_2 is not favourable, so $\beta' = 1$ and all the transmit power is allocated to node 1.

3.2.3 Cooperation or Not?

As seen in the previous sections, nodes 1 and 2 should cooperate when there exists a minimum point for $p_{out,3}$ where $\beta \in (0,1)$. (Note that it is an open interval.) Actually, we can determine whether cooperation should be done without finding the optimal β numerically in advance. We first compute the first derivative of $p_{out,3}$ which is given by

$$\frac{dp_{out,3}}{d\beta} = \begin{cases} \frac{k^2(d_1^\alpha+d_2^\alpha)^3(d_1^\alpha-d_2^\alpha)}{2d_1^\alpha d_2^\alpha}\exp[-k(d_1^\alpha+d_2^\alpha)] & \text{for } \beta = \frac{d_1^\alpha}{d_1^\alpha+d_2^\alpha} \\ \frac{d_1^\alpha d_2^\alpha}{(1-\beta)d_1^\alpha-\beta d_2^\alpha}\left[\frac{\exp\left(-\frac{kd_1^\alpha}{\beta}\right)}{(1-\beta)d_1^\alpha-\beta d_2^\alpha} - \frac{\exp\left(-\frac{kd_2^\alpha}{1-\beta}\right)}{(1-\beta)d_1^\alpha-\beta d_2^\alpha} + \frac{k\exp\left(-\frac{kd_1^\alpha}{\beta}\right)}{\beta} + \frac{k\exp\left(-\frac{kd_2^\alpha}{1-\beta}\right)}{1-\beta}\right] & \text{otherwise} \end{cases} \tag{3.22}$$

where $k = \frac{\Theta N_0}{P}$. The following lemma and proposition help us establish the criteria for cooperation:

Lemma 1. *$\frac{dp_{out,3}}{d\beta}$ is continuous for $\beta \in (0,1)$*

Proof. It is quite obvious that $\frac{dp_{out,3}}{d\beta}$ is continuous for all the points where $\beta \in (0,1)$, except for the point $\beta = \frac{d_1^\alpha}{d_1^\alpha+d_2^\alpha}$ which requires more careful consideration. Because

$$
\begin{aligned}
&\lim_{\beta \to \frac{d_1^\alpha}{d_1^\alpha + d_2^\alpha}} \frac{dp_{out,3}}{d\beta} \\
&= \lim_{\beta \to \frac{d_1^\alpha}{d_1^\alpha + d_2^\alpha}} \frac{d_1^\alpha d_2^\alpha \begin{bmatrix} \beta(1-\beta)\exp\left(-\frac{kd_1^\alpha}{\beta}\right) - \beta(1-\beta)\exp\left(-\frac{kd_2^\alpha}{1-\beta}\right) \\ +(1-\beta)[(1-\beta)d_1^\alpha - \beta d_2^\alpha]k\exp\left(-\frac{kd_1^\alpha}{\beta}\right) \\ +\beta[(1-\beta)d_1^\alpha - \beta d_2^\alpha]k\exp\left(-\frac{kd_2^\alpha}{1-\beta}\right) \end{bmatrix}}{[(1-\beta)d_1^\alpha - \beta d_2^\alpha]^2\beta(1-\beta)} \\
&= \lim_{\beta \to \frac{d_1^\alpha}{d_1^\alpha + d_2^\alpha}} \frac{d_1^\alpha d_2^\alpha \begin{bmatrix} (1-2\beta)\exp\left(-\frac{kd_1^\alpha}{\beta}\right) + \frac{(1-\beta)kd_1^\alpha}{\beta}\exp\left(-\frac{kd_1^\alpha}{\beta}\right) \\ -(1-2\beta)\exp\left(-\frac{kd_2^\alpha}{1-\beta}\right) + \frac{\beta kd_2^\alpha}{1-\beta}\exp\left(-\frac{kd_2^\alpha}{1-\beta}\right) \\ +k\left\{ \begin{array}{l} \exp\left(-\frac{kd_1^\alpha}{\beta}\right)[-[(1-\beta)d_1^\alpha - \beta d_2^\alpha] - (1-\beta)(d_1^\alpha + d_2^\alpha)] \\ +(1-\beta)[(1-\beta)d_1^\alpha - \beta d_2^\alpha]\frac{kd_1^\alpha}{\beta^2}\exp\left(-\frac{kd_1^\alpha}{\beta}\right) \end{array} \right\} \\ +k\left\{ \begin{array}{l} \exp\left(-\frac{kd_2^\alpha}{1-\beta}\right)[[(1-\beta)d_1^\alpha - \beta d_2^\alpha] - \beta(d_1^\alpha + d_2^\alpha)] \\ -\beta[(1-\beta)d_1^\alpha - \beta d_2^\alpha]\frac{kd_2^\alpha}{(1-\beta)^2}\exp\left(-\frac{kd_2^\alpha}{1-\beta}\right) \end{array} \right\} \end{bmatrix}}{-2\beta(1-\beta)(d_1^\alpha + d_2^\alpha)[(1-\beta)d_1^\alpha - \beta d_2^\alpha] + (1-2\beta)[(1-\beta)d_1^\alpha - \beta d_2^\alpha]^2} \\
&= \frac{d_1^\alpha d_2^\alpha \exp[-k(d_1^\alpha + d_2^\alpha)]k^2(d_1^\alpha + d_2^\alpha)^2 \frac{d_1^{2\alpha} - d_2^{2\alpha}}{d_1^\alpha d_2^\alpha}}{2d_1^\alpha d_2^\alpha} \\
&= \frac{k^2(d_1^\alpha + d_2^\alpha)^3(d_1^\alpha - d_2^\alpha)}{2d_1^\alpha d_2^\alpha}\exp[-k(d_1^\alpha + d_2^\alpha)]
\end{aligned}
\tag{3.23}
$$

So, $\frac{dp_{out,3}}{d\beta}$ is continuous for all the points where $\beta \in [0,1]$. The 2nd and 3rd lines are obtained by applying L'Hospital's Rule to $\frac{0}{0}$ forms. □

We then define the transmit SNR for each hop to be P/N_0 and let the distances between nodes 1 and 2 to the node T be d_1 and d_2 respectively.

Proposition 2. *A minimum point exists for $p_{out,3}$ for $\beta \in (0,1)$ if $\frac{Pd_1^{-\alpha}}{N_0} > \Theta$ and $\frac{Pd_2^{-\alpha}}{N_0} > \Theta$.*

Proof. Consider the $p_{out,3}$ against β graph, it is smooth and is continuously differentiable and its 1st derivative, $\frac{dp_{out,3}}{d\beta}$, is continuous (proved in Lemma 1). If the slope

(or 1st derivative of $p_{out,3}$) near β=0 is negative and that near β=1 is positive (i.e. $\lim_{\beta\to 0^+} \frac{dp_{out,3}}{d\beta} < 0$ and $\lim_{\beta\to 1^-} \frac{dp_{out,3}}{d\beta} > 0$), by Bolzano's Intermediate Value Theorem [3], there exists a value such that the slope is equal to zero, i.e. a minimum point exists for $p_{out,3}$ in the interval of $\beta \in (0,1)$.

Evaluating $\lim_{\beta\to 0^+} \frac{dp_{out,3}}{d\beta} < 0$ and $\lim_{\beta\to 1^-} \frac{dp_{out,3}}{d\beta} > 0$, we have

$$
\begin{aligned}
&\lim_{\beta\to 0^+} \frac{dp_{out,3}}{d\beta} \\
&= \lim_{\beta\to 0^+} \frac{d_1^\alpha d_2^\alpha}{(1-\beta)d_1^\alpha - \beta d_2^\alpha} \left[\frac{\exp\left(-\frac{kd_1^\alpha}{\beta}\right)}{(1-\beta)d_1^\alpha - \beta d_2^\alpha} - \frac{\exp\left(-\frac{kd_2^\alpha}{1-\beta}\right)}{(1-\beta)d_1^\alpha - \beta d_2^\alpha} + \frac{k\exp\left(-\frac{kd_1^\alpha}{\beta}\right)}{\beta} + \frac{k\exp\left(-\frac{kd_2^\alpha}{1-\beta}\right)}{1-\beta} \right] \\
&= d_2^\alpha \left[\lim_{\beta\to 0^+} \frac{1}{d_1^\alpha \exp\left(\frac{kd_1^\alpha}{\beta}\right)} - \frac{1}{d_1^\alpha \exp\left(kd_2^\alpha\right)} + \lim_{\beta\to 0^+} \frac{k}{\beta \exp\left(\frac{kd_1^\alpha}{\beta}\right)} + \frac{k}{\exp\left(kd_2^\alpha\right)} \right] \\
&= d_2^\alpha \left[-\frac{1}{d_1^\alpha \exp\left(kd_2^\alpha\right)} + \frac{k}{\exp\left(kd_2^\alpha\right)} \right] \\
&= \frac{d_2^\alpha}{e^{kd_2^\alpha}} \left[-\frac{1}{d_1^\alpha} + \frac{\Theta N_0}{P} \right] < 0 \\
&\Leftrightarrow \frac{P d_1^{-\alpha}}{N_0} > \Theta
\end{aligned}
\tag{3.24}
$$

and

$$
\begin{aligned}
&\lim_{\beta\to 1^-} \frac{dp_{out,3}}{d\beta} \\
&= \lim_{\beta\to 1^-} \frac{d_1^\alpha d_2^\alpha}{(1-\beta)d_1^\alpha - \beta d_2^\alpha} \left[\frac{\exp\left(-\frac{kd_1^\alpha}{\beta}\right)}{(1-\beta)d_1^\alpha - \beta d_2^\alpha} - \frac{\exp\left(-\frac{kd_2^\alpha}{1-\beta}\right)}{(1-\beta)d_1^\alpha - \beta d_2^\alpha} + \frac{k\exp\left(-\frac{kd_1^\alpha}{\beta}\right)}{\beta} + \frac{k\exp\left(-\frac{kd_2^\alpha}{1-\beta}\right)}{1-\beta} \right] \\
&= -d_1^\alpha \left[-\frac{1}{d_2^\alpha \exp\left(kd_1^\alpha\right)} + \lim_{\beta\to 1^-} \frac{1}{d_2^\alpha \exp\left(\frac{kd_2^\alpha}{1-\beta}\right)} + \frac{k}{\exp\left(kd_1^\alpha\right)} + \lim_{\beta\to 1^-} \frac{k}{(1-\beta)\exp\left(\frac{kd_2^\alpha}{1-\beta}\right)} \right] \\
&= -d_1^\alpha \left[-\frac{1}{d_2^\alpha \exp\left(kd_1^\alpha\right)} + \frac{k}{\exp\left(kd_1^\alpha\right)} \right] \\
&= \frac{d_1^\alpha}{e^{kd_1^\alpha}} \left[+\frac{1}{d_2^\alpha} - \frac{\Theta N_0}{P} \right] > 0 \\
&\Leftrightarrow \frac{P d_2^{-\alpha}}{N_0} > \Theta
\end{aligned}
\tag{3.25}
$$

□

As our goal is to minimize $p_{out,3}$, we should cooperate if the optimal β which

minimizes $p_{out,3}$ lies in the open interval of (0,1). As suggested in proposition 2, the criteria for cooperation are $\frac{Pd_1^{-\alpha}}{N_0} > \Theta$ and $\frac{Pd_2^{-\alpha}}{N_0} > \Theta$. If we define the transmission radius r at a particular transmit SNR to be $r = \left(\frac{P}{\Theta N_0}\right)^{\frac{1}{\alpha}}$, then the criteria of cooperation are $d_1 < r$ and $d_2 < r$. It means that the receiver T is within the transmission radii of both nodes 1 and 2.

3.3 Performance Analysis and Evaluation

In this section, we are going to evaluate the outage performance of some simple cooperative strategies in 1D random network and grid network. Analyses and simulation results are provided.

3.3.1 1D Poisson Random Network

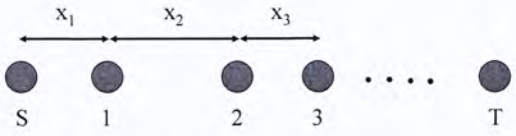

Figure 3.3: 1D Poisson random network.

We first study cooperative routing in a 1-dimensional Poisson random network with density λ. From [18], the probability density function of Euclidean distance to the nearest neighbour on the right (or left) side R_1 is given by

$$p_{R_1}(x) = \lambda e^{-\lambda x} \text{ for } x \geq 0 \tag{3.26}$$

Consider the 1D linear network in Fig. 3.3, where x_i is the distance between node i and its nearest neighbour on the left. Suppose that the node S is the source and node T is the sink. We compare transmission schemes with or without cooperation. For non-cooperative schemes, packets are sent from S to T hop by hop (i.e. $S \rightarrow 1 \rightarrow 2 \rightarrow 3 \rightarrow \ldots \rightarrow T$). For cooperative schemes, a node and its nearest neighbour

on the left cooperatively send packets to its nearest neighbour on the right (i.e. node S cooperates with node 1 to send to node 2, node 1 cooperates with node 2 to send to node 3 ...). However, it should be noticed that the first hop from node S to node 1 is always non-cooperative, even in the cooperative scheme.

In this setup, we define successful reception in each hop to be the event that the receiver is in the transmission radius of the transmitter AND that the receive SNR per bit γ_b is larger than the threshold Θ. The successful reception for the whole route is defined to be the event that receptions are successful for all the hops along the route. However, because the first hop from node S to node 1 is always non-cooperative, we exclude the first hop in our calculation.

Mathematically, let S_i be the event that receiver is in the transmission radius of the transmitter in the ith hop and T_i be the event that receiver receives the signal with $\gamma_b \geq \Theta$ in the ith hop. Let $p_{r,i}$ be the reception probability for the ith hop. We have

$$\begin{aligned} &P(S_1) = P(S_2) = ... = P(S_n) \\ &= P(R_1 < r) = \int_0^r \lambda e^{-\lambda x} dx = 1 - e^{-\lambda r} \end{aligned} \tag{3.27}$$

Reception probability for a route with n hops given that the first hop is successful is given by

$$\begin{aligned} &p_{r,route} = p(S_1, S_2, ..., S_n, T_1, T_2, ..., T_n | S_1, T_1) \\ &= p(S_2, ..., S_n, T_2, ..., T_n | S_1, T_1) \\ &= p(S_2, ..., S_n) p(T_2, ..., T_n | S_2, ..., S_n, S_1, T_1) \\ &= p(S_2) ... p(S_n) p(T_2, ..., T_n | S_2, ..., S_n, S_1, T_1) \\ &= (1 - e^{-\lambda r})^{n-1} \int_0^r ... \int_0^r \prod_{i=2}^n p_{r,i} \prod_{i=1}^n \frac{p_{R_1}(x_i)}{1 - e^{-\lambda r}} dx_1 ... dx_n \\ &= (1 - e^{-\lambda r})^{-1} \int_0^r ... \int_0^r \prod_{i=2}^n p_{r,i} \prod_{i=1}^n p_{R_1}(x_i) dx_1 ... dx_n \\ &= 1 - p_{out,route} \end{aligned} \tag{3.28}$$

where $p_{out,route}$ is the probability of outage for the route given that the first hop is

successful. The third line of the equation is due to the fact that the two sets of events $\{S_2, \ldots, S_n\}$ and $\{S_1, T_1\}$ are independent, while the fourth line is the result of the independence of events $S_2, \ldots, S_n$.

For non-cooperation, we have

$$p_{r,i} = \exp(-kx_i^{\alpha}) \text{ for } i = 2,\ldots,n. \tag{3.29}$$

For cooperation, we have

$$p_{r,i} = \frac{(1-\beta_i)x_i^{\alpha}}{(1-\beta_i)x_i^{\alpha}-\beta_i(x_{i-1}+x_i)^{\alpha}} \exp\left(-\frac{k(x_{i-1}+x_i)^{\alpha}}{(1-\beta_i)}\right) - \frac{\beta_i(x_{i-1}+x_i)^{\alpha}}{(1-\beta_i)x_i^{\alpha}-\beta_i(x_{i-1}+x_i)^{\alpha}} \exp\left(-\frac{kx_i^{\alpha}}{\beta_i}\right) \tag{3.30}$$

for $i = 2,\ldots,n$ and β_i is the power distribution ratio between the two signals traveling through distances x_i and $x_{i-1} + x_i$ and it depends on the values of x_{i-1}, x_i and k.

For $n = 3$, the result of analysis and simulation are shown in Fig. 3.4. We see that the cooperative scheme achieves a diversity order of two at high transmit SNR.

3.3.2 2D Grid Network

Consider a 2D network as shown in Fig. 3.5. Assume that node S is the source and node T is the sink. The distance between the nearest neighbour is d and that between diagonal nodes is $\sqrt{2}d$. We first need to find a good single path route that serves as the basis of the cooperative route. Short hop route is a reasonable choice as stated by the proposition below. Given S and T, short hop routes refer to the routes which take a larger number of hops between S and T. The distance between the sender and receiver in each hop is short. Long hop routes are the routes that choose the opposite approach and take a smaller number of hops. The distance between the sender and receiver in each hop is long. In the following proposition, we define long hop route to be the route with only one transmission directly from S to T and short hop route to be the route with n-hop transmissions when there are n equal-distance hops in between S and T.

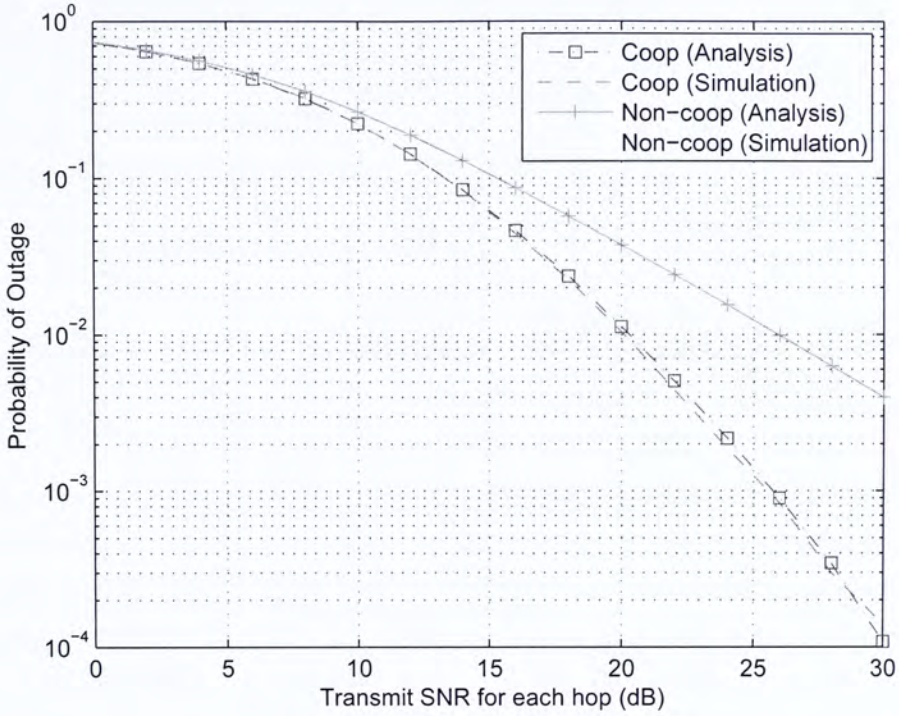

Figure 3.4: Probability of outage vs. transmit SNR in 1D random network for $n = 3$.

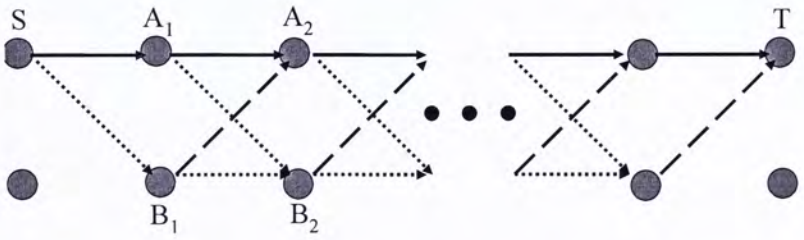

Figure 3.5: 2D grid network.

Proposition 3. *In a linear network, short hop routing has a lower probability of outage than long hop routing when path loss exponent $\alpha > 2$.*

Proof. The probability of outage for a route is given by

$$p_{out,route} = 1 - \prod_{i=1}^{n} p_{r,i} = 1 - e^{-R_{tot}} \tag{3.31}$$

Assume that the distance between the source and destination is d and the total power constraint is P_0. For a n-hop transmission which the transmission distance for each hop is the same,

$$R_{tot} = n\frac{\Theta N_0(\frac{d}{n})^\alpha}{\frac{P_0}{n}} = \frac{kd^\alpha}{n^{\alpha-2}} \tag{3.32}$$

where $k = \frac{\Theta N_0}{P_0}$. For $\alpha > 2$, the larger the number of hops n, the smaller the R_{tot}, the smaller the $p_{out,route}$. □

By proposition 3, it is reasonable to do a short hop routing from S to T to have a low probability of outage, which we assume that there are n short hops in between. Let P be the transmit power constraint for each hop. For non-cooperative routing, packets are sent from S hop by hop to T. For cooperative routing, we assume that the same cooperative route is used for all transmit power level that cooperative node B_i will cooperate with node A_i to transmit in hop i+1 if node B_i can correctly overhear the message in the previous hop, as shown in Fig. 3.5. We denote the original non-cooperative transmissions by solid lines, additional transmissions due to cooperation by dashed lines and unintended transmissions due to broadcast nature of wireless communication (Wireless Multicast Advantage) by dotted lines. In cooperative routing, cooperative node B_i will only cooperate with node A_i if B_i can overhear the message correctly in the previous hop (i.e. receive $\gamma_b \geq \Theta$). In other words, although nodes A_i and B_i are designated as cooperative partners in the cooperative route, they will not transmit cooperatively unless B_i overhears the message with receive $\gamma_b \geq \Theta$.

Let dist(A,B) be the Euclidean distance between nodes A and B. We first define reception probability at the receiver when node A and B transmit with power of

βP and $(1-\beta)P$ respectively, given that nodes A and B have received the message correctly

$$f(\beta, d_1, d_2) = \frac{(1-\beta)d_1^\alpha}{(1-\beta)d_1^\alpha - \beta d_2^\alpha} \exp\left(-\frac{kd_2^\alpha}{(1-\beta)}\right) - \frac{\beta d_2^\alpha}{(1-\beta)d_1^\alpha - \beta d_2^\alpha} \exp\left(-\frac{kd_1^\alpha}{\beta}\right) \tag{3.33}$$

where $d_1 = \text{dist(A,T)}$, $d_2 = \text{dist(B,T)}$ and $k = \frac{\Theta N_0}{P}$.

Let β_1 be an optimal (or near optimal) power distribution for $d_1 = d$ and $d_2 = \sqrt{2}d$, which minimizes the function f.

We then proceed to analyze the performance of non-cooperative and cooperative routing. Let $p_{r,i}$ be the reception probability for the ith hop for $i = 1,\ldots,n$ and H_i be the event that cooperative node B_i can overhear the message correctly in the previous hop for $i = 1,\ldots,n$. We aim to compare the end-to-end probability of outage for the route given that the first hop is successful which is given by $p_{out,route} = 1 - \prod_{i=2}^{n} p_{r,i}$. The first hop is excluded in our calculation, because it is always non-cooperative even in cooperative schemes, and thus reduces the difference in performance between cooperative and non-cooperative schemes.

For non-cooperative routing, we have

$$p_{r,1} = p_{r,2} = \ldots = p_{r,n} = \exp(-kd^\alpha) \tag{3.34}$$

For cooperative routing, we have

$$p_{r,1} = \exp(-kd^\alpha) \tag{3.35}$$

$$\begin{aligned} p_{r,i} &= \text{P(reception|not } H_i)\text{P(not } H_i) + \text{P(reception}|H_i)\text{P}(H_i) \\ &= \exp(-kd^\alpha)[1 - P(H_i)] + f(\beta_1, d, \sqrt{2}d)P(H_i) \end{aligned} \tag{3.36}$$

for $i = 2,\ldots,n$. $P(H_i)$ can be computed recursively in the following way:

$$P(H_2) = \exp(-k(\sqrt{2}d)^\alpha) \tag{3.37}$$

$$\begin{aligned} P(H_i) &= \text{P}(H_i|\text{not } H_{i-1})\text{P(not } H_{i-1}) + \text{P}(H_i|H_{i-1})\text{P}(H_{i-1}) \\ &= \exp(-k(\sqrt{2}d)^\alpha)[1 - P(H_{i-1})] + f(\beta_1, \sqrt{2}d, d)P(H_{i-1}) \end{aligned} \tag{3.38}$$

for $i = 3,\ldots,n$. The results of analysis and simulation are given in Fig. 3.6 for $n = 10$, $d = 1$ and $\alpha = 4$. We see that the cooperative scheme achieves a diversity order of two at high transmit SNR.

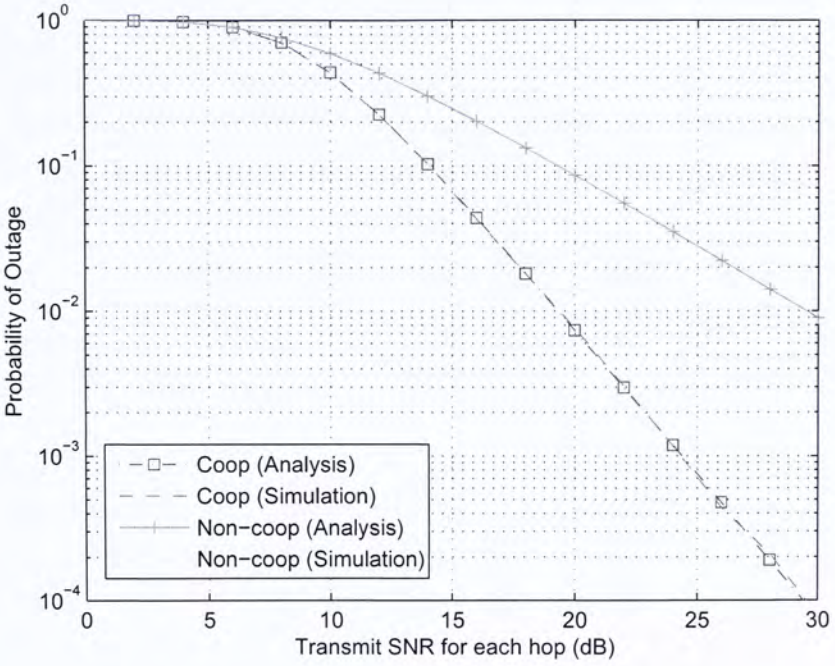

Figure 3.6: Probability of outage vs. transmit SNR in 2D grid network for $n = 10$.

3.4 Cooperative Routing Algorithm

In this section, we are interested to form a route with diversity order of two, so that it has a lower probability of outage. Our cooperative routing algorithm is suggested and simulation result in 2D Poisson random network is given.

3.4.1 Cooperative Routing Algorithm

When using our cooperative routing algorithm, a single path route needs to be given first. Then our algorithm is applied to decide on cooperative partner, power distribution ratio and transmission protocol in each hop, so as to reduce the probability of outage of the original single path route.

Let d_1 = dist(A,T), d_2 = dist(B,T) and $k = \frac{\Theta N_0}{P}$. The reception probability at the receiver when nodes A and B transmit with power of βP and $(1-\beta)P$ respectively, given that nodes A and B have received the message correctly, is given by the following function

$$f(\beta, d_1, d_2, k) = \frac{(1-\beta)d_1^\alpha}{(1-\beta)d_1^\alpha - \beta d_2^\alpha} \exp\left(-\frac{kd_2^\alpha}{(1-\beta)}\right) - \frac{\beta d_2^\alpha}{(1-\beta)d_1^\alpha - \beta d_2^\alpha} \exp\left(-\frac{kd_1^\alpha}{\beta}\right) \tag{3.39}$$

Based on the results in the previous sections, our cooperative routing algorithm is as follows:

Step 1: (Input)

A single path route **S** is first generated e.g. **S** = [1 2 3 4] and we define l to be the number of elements in **S**.

Step 2: (Initialization)

We then initialize a cooperative route by creating a matrix **C** with dimension $2 \times l$, of which the upper row is identical to **S** and the lower row is filled with zeros. E.g. $C = \begin{pmatrix} 1 & 2 & 3 & 4 \\ 0 & 0 & 0 & 0 \end{pmatrix}$. The number of hops $n = l - 1$. If the total power constraint for the route is P_0, then the transmit power for each hop is P_0/n.

Step 3: (Cooperative Route Formation)

Run the following pseudo code:

1. $i = 1$.

2. Power distribution ratio for hop 1: $\beta_1 = 1$.

3. While $(i < n)$ do

   (a) Define h_1 =**C**(1,i); h_2 =**C**(2,i); m=**C**(1,i+1); t=**C**(1,i+2).

   (b) Find a set of nodes x, which is within the transmission radius of h_1 (and h_2 if it exists) given a certain power distribution β_i AND that the next hop node t is within its transmission radius. Specifically, we want to find node x, which

$$\frac{P_i d_1^{-\alpha}}{N_0} \geq \Theta \text{ for } h_2 = 0 \tag{3.40}$$

$$\frac{\beta_i P_i d_1^{-\alpha} + (1-\beta_i) P_i d_2^{-\alpha}}{N_0} \geq \Theta \text{ for } h_2 \neq 0 \tag{3.41}$$

$$\frac{P_{i+1} d_3^{-\alpha}}{N_0} \geq \Theta \tag{3.42}$$

   where d_1 = dist(x, h_1); d_2 = dist(x, h_2); d_3 = dist(x, t). Put x into a set **D**.

   (c) Find $w \in \mathbf{D}$, which has the maximum value of probability of reception $p_{r,i+1}$ in the $i+1$th hop. Because $p_{r,i+1}$ = P(reception | cooperation in ith hop)P(cooperation in ith hop) + P(reception | non-cooperation in ith hop)P(non-cooperation in ith hop), its value is given by:

   For $h_2 = 0$, we have

$$p_r = f(\beta_{i+1}, d_4, d_1, k_{i+1}) \exp(-k_i d_2^{\alpha}) + \exp(-k_{i+1} d_4^{\alpha})[1 - \exp(-k_i d_2^{\alpha})] \tag{3.43}$$

   For $h_2 \neq 0$ and assume that cooperative communication is used in the previous hop, we have

$$p_r = f(\beta_{i+1}, d_4, d_1, k_{i+1}) f(\beta_i, d_2, d_3, k_i) + \exp(-k_{i+1} d_4^{\alpha})[1 - f(\beta_i, d_2, d_3, k_i)] \tag{3.44}$$

   where d_1 = dist(w,t); d_2 = dist(w,h_1); d_3 = dist(w, h_2), d_4 = dist(m,t); $k_i = \frac{\Theta N_0}{P_i}$.

(d) Set **C**(2, i+1) = w.

(e) Calculate β_{i+1}, which is the optimal power distribution for transmission distances dist(m,t) and dist(w,t).

(f) $i = i + 1$.

Step 4: (Transmission)

For each hop i, if **C**(2, i) $\neq 0$, node **C**(2, i) should cooperate with **C**(1, i) and transmit to node **C**(1, i+1), if node **C**(2, i) can overhear the message in the previous hop correctly (i.e. receive $\gamma_b \geq \Theta$). The transmit power distribution ratio of **C**(1, i) to **C**(2, i) is β_i. Although **C**(1, i) and **C**(2, i) are designated as partners for cooperation in step 3, they will not transmit cooperatively if **C**(2, i) cannot overhear the message sent in the previous hop correctly.

3.4.2 2D Random Network

We evaluate our cooperative routing algorithm in a 30m $\times$ 30m network with 30 nodes, which are randomly distributed in the area for each network realization. We consider routes that their number of hops is between two to four. Outage for the route occurs when any one of the hops along the route has receive $\gamma_b < \Theta$. In our evaluation, we consider probability of outage given the first hop is successful, because the first hop is always non-cooperative. After running 100000 iterations for each of the 50 different network realizations we consider, the result is shown in Fig. 3.7. We see that our cooperative routing algorithm can achieve a diversity order of two at high transmit SNR.

□ **End of chapter.**

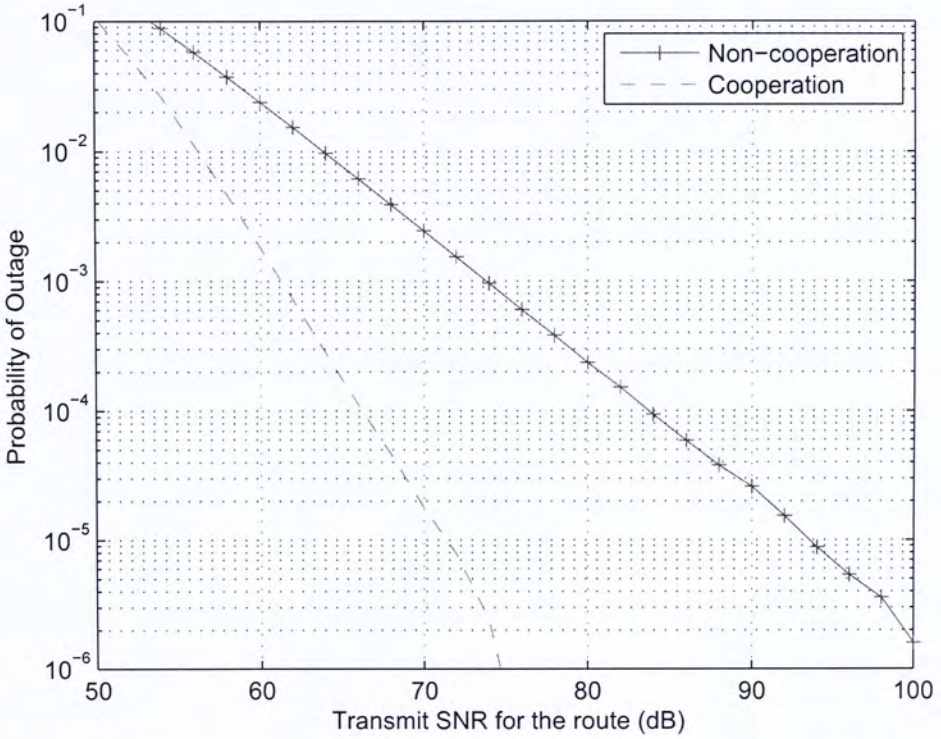

Figure 3.7: Probability of outage vs. transmit SNR in 2D random networks.

Chapter 4

UWB System Model and BER Expression

In this chapter, we introduce the UWB system model that we use in our work. In particular, Pulse Position Modulation (PPM) - Time Hopping (TH) - UWB is used for transmission and Rake receiver is useful for reception. Saleh-Valenzuela (S-V) model is used to model the indoor multipath channel. We consider transmission in the presence of both Multi-User Interference (MUI) and Additive White Gaussian Noise (AWGN). Based on [48], [5] and [12], we evaluate the BER expression of Rake receiver in both MUI and AWGN. In fact, [48] and [5] have found the BER expression for PPM-TH-UWB in MUI and AWGN, without using Rake receiver. [12] considers single-user binary block-code PPM transmission using Rake receiver in the absence of MUI. We evaluate the performance of different types of Rake receivers in different levels of interference. Some simple short-hop and long hop routing strategies are also compared.

4.1 Transmit Signal

We apply binary Pulse Position Modulation(PPM) - Time Hopping(TH) - UWB for transmission ([38], [47] and [48]). The transmitted signal is of the form:

$$s^{(k)}(t) = A^{(k)} \sum_{j=-\infty}^{\infty} p(t - jT_f - c_j^{(k)} T_c - \delta d_{\lfloor j/N_s \rfloor}^{(k)}) \tag{4.1}$$

where $A^{(k)}$ is amplitude which controls the transmitted power for the kth user. $p(t)$ is the transmitted pulse. We assume that it is defined in $[0, T_p]$ and thus its pulse width is T_p. Moreover, we assume that $\int_0^{T_p} p^2(t)dt = 1$ and $\int_0^{T_p} p(t)dt = 0$. T_f is the pulse repetition time (or called frame duration). $\{c_j^{(k)}\}$ is the time-hopping sequence for the kth user. We assume that the TH code is a sequence of N_p independent and identical random variables with a probability of $1/N_h$ in taking one of the integer values in the range [0, N_h-1]. T_c is the duration of addressable time delay bins (or called chip duration). δ is the time shift used to distinguish between pulses carrying the bit 0 and the bit 1. $\{d_{\lfloor j/N_s \rfloor}^{(k)}\}$ is the binary information stream for the kth user. We assume that the bit period $T_b = N_s T_f$, $T_f = N_h T_c$ and $T_c \geq \delta + T_p$.

Consider only a bit interval which $0 \leq t \leq T_b$. The transmitted signal is simplified as

$$s^{(k)}(t) = A^{(k)} \sum_{j=0}^{N_s - 1} p(t - jT_f - c_j^{(k)} T_c - \delta d_j^{(k)}) \tag{4.2}$$

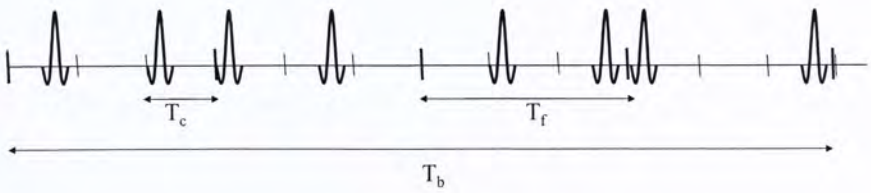

Figure 4.1: PPM-TH-UWB with $N_s = 4$ and $N_h = 3$: User 1 is sending the bit 0, using the time-hopping sequence {2, 0, 1, 0}, while user 2 is sending the bit 1, using the time-hopping sequence {0, 1, 2, 2}.

4.2 Channel Model

We adopt the Salch-Valenzuela (S-V) model [27] in modeling the indoor multipath channel, which the multipath components arrive at the receiver in clusters. The channel for the kth user is

$$h^{(k)}(t) = X^{(k)} \sum_{l=1}^{L^{(k)}} \sum_{q=1}^{Q^{(k)}(l)} \alpha_{q,l}^{(k)} \delta(t - T_l^{(k)} - \tau_{q,l}^{(k)} - \zeta^{(k)}) \tag{4.3}$$

where $X^{(k)}$ the amplitude gain of the channel due to log-normal shadowing for the kth user. $L^{(k)}$ is the number of observed clusters and $Q^{(k)}(l)$ is the number of multipath components received within the lth cluster. $\alpha_{q,l}^{(k)}$ is the multipath gain coefficient for the qth multipath component in the lth cluster for the kth user. $T_l^{(k)}$ is the delay of the lth cluster and $\tau_{q,l}^{(k)}$ is the delay of the qth multipath component relative to the lth cluster arrival time for the kth user. $T_l^{(k)}$ and $\tau_{q,l}^{(k)}$ are modeled by two Poisson processes with different rates. $\zeta^{(k)}$ is the random time delay for the kth user which is uniformly distributed over the interval $[0, T_f]$. For notational simplicity, we replace $T_l^{(k)}$ and $\tau_{q,l}^{(k)}$ with $\tau_m^{(k)}$. The channel is thus represented by

$$h^{(k)}(t) = X^{(k)} \sum_{m=1}^{M^{(k)}} \alpha_m^{(k)} \delta(t - \tau_m^{(k)} - \zeta^{(k)}) \tag{4.4}$$

where $M^{(k)}$ is the total number of multipath components produced by the transmission of user k.

4.3 Received Signal

Assume that bit "0" is sent by the transmitter. Let N be the total number of transmitters in the system, where $N-1$ of them are undesired users. Assuming that there is a perfect synchronization between transmitter 1 and the reference receiver, i.e. $\zeta^{(1)}$ is known by the receiver and that $\zeta^{(1)} = 0$. The composite received signal at the output of the receiver's antenna is modeled as

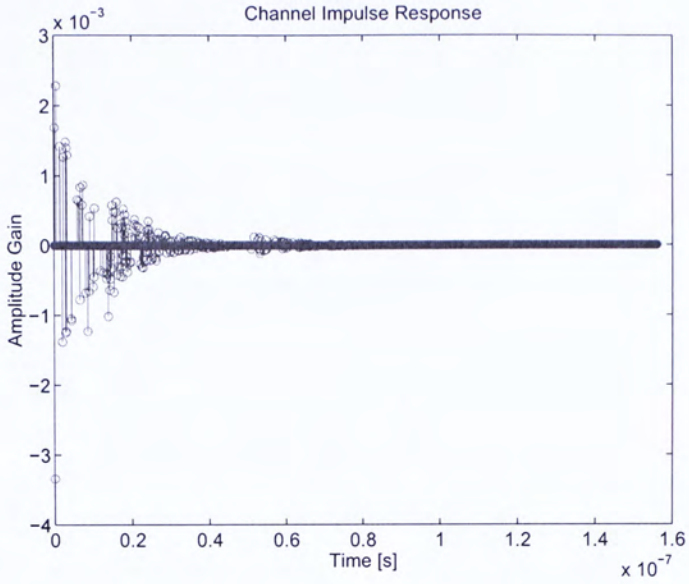

Figure 4.2: UWB Channel Impulse Response.

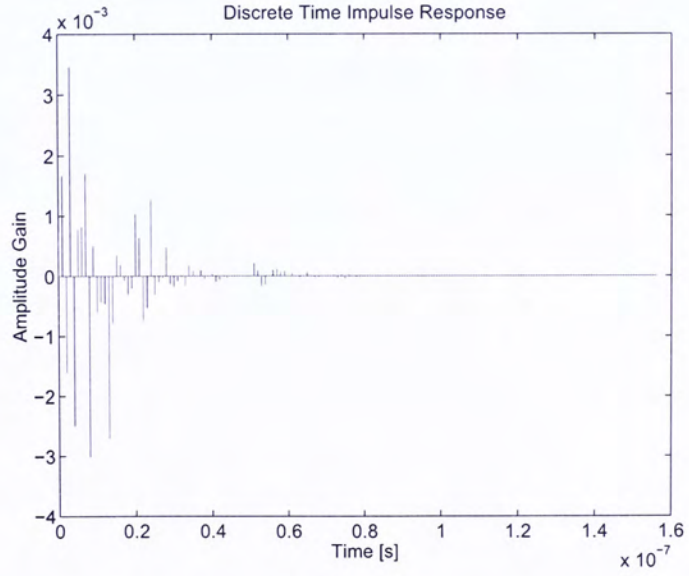

Figure 4.3: UWB Discrete Time Channel Impulse Response.

$$\begin{aligned} r(t) &= \sum_{k=1}^{N} s^{(k)}(t) * h^{(k)}(t) + n(t) \\ &= r_u(t) + r_{mui}(t) + n(t) \end{aligned} \tag{4.5}$$

with

$$\begin{aligned} r_u(t) &= s^{(1)}(t) * h^{(1)}(t) \\ &= A^{(1)} X^{(1)} \sum_{j=0}^{N_s-1} \sum_{m=1}^{M^{(1)}} \alpha_m^{(1)} p(t - jT_f - c_j^{(1)} T_c - \tau_m^{(1)}) \end{aligned} \tag{4.6}$$

$$\begin{aligned} r_{mui}(t) &= \sum_{k=2}^{N} s^{(k)}(t) * h^{(k)}(t) \\ &= \sum_{k=2}^{N} A^{(k)} X^{(k)} \sum_{j=0}^{N_s-1} \sum_{m=1}^{M^{(k)}} \alpha_m^{(k)} p(t - jT_f - c_j^{(k)} T_c - \delta d_j^{(k)} - \tau_m^{(k)} - \zeta^{(k)}) \end{aligned} \tag{4.7}$$

where $n(t)$ is a zero mean, AWGN random process with two-sided power spectral density $N_0/2$.

4.4 Rake Receiver with Maximal-Ratio Combining (MRC)

Assume the receiver is a L-finger Rake with perfect channel estimation and it is synchronized with transmitter 1. The correlation receiver mask used for reception is a sequence of pulses placed at the designated position according to the timing information of PPM-TH-UWB system

$$\begin{aligned} m(t) &= \sum_{j=0}^{N_s-1} p(t - jT_f - c_j^{(1)} T_c) - p(t - jT_f - c_j^{(1)} T_c - \delta) \\ &= \sum_{j=0}^{N_s-1} v(t - jT_f - c_j^{(1)} T_c) \end{aligned} \tag{4.8}$$

with the receiver template $v(t) = p(t) - p(t - \delta)$. We take $\delta = T_p$ for orthogonal PPM.

For the finger indexed by l, the decision variable is

$$\begin{aligned} Z_l &= \int_0^{T_b} r(t) m(t - \tau_l) dt \\ &= Z_{u,l} + Z_{mui,l} + Z_{n,l} \end{aligned} \tag{4.9}$$

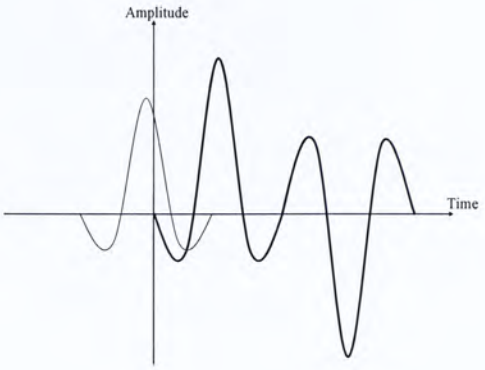

Figure 4.4: The presence of an interfering pulse (thin line) at the receiver input will lead to interference, obtained by multiplication and then integration with the receiver template (thick line) $v(t) = p(t) - p(t - T_p)$.

where the decision variables due to the useful signal part, MUI and noise are given by

$$Z_{u,l} = \int_0^{T_b} r_u(t)m(t - \tau_l)dt \tag{4.10}$$

$$Z_{mui,l} = \int_0^{T_b} r_{mui}(t)m(t - \tau_l)dt \tag{4.11}$$

$$Z_{n,l} = \int_0^{T_b} n(t)m(t - \tau_l)dt \tag{4.12}$$

For the signal part $Z_{u,l}$, with perfect channel estimation, the Rake receiver can set $\tau_l = \tau_m^{(1)}$ to track the multipath component with delay $\tau_m^{(1)}$ and amplitude gain $\alpha_m^{(1)}$. So the amplitude of the multipath component tracked by the lth finger is $\alpha_l = \alpha_m^{(1)}$.

$$
\begin{aligned}
Z_{u,l} &= \int_0^{T_b} r_u(t)m(t-\tau_l)dt \\
&= A^{(1)}X^{(1)} \int_0^{T_b} \sum_{j=0}^{N_s-1} \alpha_l p(t-jT_f-c_j^{(1)}T_c-\tau_l) \sum_{k=0}^{N_s-1} v(t-kT_f-c_k^{(1)}T_c-\tau_l)dt \\
&= A^{(1)}X^{(1)} \int_0^{T_b} \sum_{j=0}^{N_s-1} \alpha_l p(t-jT_f-c_j^{(1)}T_c-\tau_l)[p(t-jT_f-c_j^{(1)}T_c-\tau_l) \\
&\qquad -p(t-jT_f-c_j^{(1)}T_c-\tau_l-T_p)]dt \\
&= A^{(1)}X^{(1)}\alpha_l \sum_{j=0}^{N_s-1} \int_{-jT_f-c_j^{(1)}T_c-\tau_l}^{T_b-jT_f-c_j^{(1)}T_c-\tau_l} p(t)[p(t)-p(t-T_p)]dt \\
&= \sqrt{E_{RX}^{(1)}}N_s\alpha_l
\end{aligned}
\tag{4.13}
$$

where the received energy from transmitter k is $E_{RX}^{(k)} = (A^{(k)}X^{(k)})^2$. The 3rd line of the equation is obtained, because a received pulse can only contribute when it is placed at the correct position of receiver mask $m(t)$.

For the noise part $Z_{n,l}$, by Gaussian Approximation, we assume the $Z_{n,l} \sim \mathcal{N}(0, \sigma_{n,l}^2)$.

$$
\begin{aligned}
Z_{n,l} &= \int_0^{T_b} n(t)m(t-\tau_l)dt \\
&= \sum_{j=0}^{N_s-1} \int_0^{T_b} n(t)[p(t-jT_f-c_j^{(1)}T_c-\tau_l)-p(t-jT_f-c_j^{(1)}T_c-\tau_l-T_p)]dt
\end{aligned}
\tag{4.14}
$$

Because $p(t)$ is an unit energy pulse, we have $Var[\int_0^{T_b} n(t)p(t-\varepsilon)dt] = \frac{N_0}{2}$ for any $0 \le \epsilon \le T_b$. Therefore

$$
\begin{aligned}
\sigma_{n,l}^2 &= Var[Z_{n,l}] \\
&= \sum_{j=0}^{N_s-1} Var\left[\int_0^{T_b} n(t)[p(t-jT_f-c_j^{(1)}T_c-\tau_l)\right] \\
&+ \sum_{j=0}^{N_s-1} Var\left[\int_0^{T_b} n(t)[p(t-jT_f-c_j^{(1)}T_c-\tau_l-T_p)\right] \\
&= N_s\tfrac{N_0}{2} + N_s\tfrac{N_0}{2} \\
&= N_sN_0
\end{aligned}
\tag{4.15}
$$

The 2nd line is obtained because the two parts in (4.14) are independent when orthogonal PPM is used [5].

For the interference part $Z_{mui,l}$, also by Gaussian Approximation, we assume that $Z_{mui,l} \sim \mathcal{N}(0, \sigma^2_{mui,l})$

$$\begin{aligned} Z_{mui,l} &= \int_0^{T_b} r_{mui}(t) m(t-\tau_l) dt \\ &= \sum_{k=2}^{N} \sum_{j=0}^{N_s-1} \sqrt{E^{(k)}_{RX}} \int_0^{T_b} \sum_{m=1}^{M^{(k)}} \alpha^{(k)}_m p(t - jT_f - c^{(k)}_j T_c - \delta d^{(k)}_j - \tau^{(k)}_m - \zeta^{(k)}) \\ &\qquad v(t - jT_f - c^{(1)}_j T_c - \tau_l) dt \end{aligned} \tag{4.16}$$

From the expression above, we observe that the interference at the output of the receiver provoked by the presence of one alien pulse transmitted by user k is given by the term inside the summation and we denote it by

$$\begin{aligned} & mui^{(k)}_p \\ &= \sqrt{E^{(k)}_{RX}} \int_0^{T_b} \sum_{m=1}^{M^{(k)}} \alpha^{(k)}_m p(t - jT_f - c^{(k)}_j T_c - \delta d^{(k)}_j - \tau^{(k)}_m - \zeta^{(k)}) \\ &\qquad v(t - jT_f - c^{(1)}_j T_c - \tau_l) dt \\ &= \sqrt{E^{(k)}_{RX}} \int_{-jT_f - c^{(1)}_j T_c - \tau_l}^{T_b - jT_f - c^{(1)}_j T_c - \tau_l} \sum_{m=1}^{M^{(k)}} \alpha^{(k)}_m p(t - \delta d^{(k)}_j - \tau^{(k)}_m - \zeta^{(k)} + \tau_l) v(t) dt \\ &= \sqrt{E^{(k)}_{RX}} \int_0^{2T_p} \sum_{m=1}^{M^{(k)}} \alpha^{(k)}_m p(t - \tau^{(k)}_m - \tau^{(k)}) v(t) dt \end{aligned} \tag{4.17}$$

where $\tau^{(k)} = \tau_l - \delta d^{(k)}_j - \zeta^{(k)}$ accounts for the delay besides $\tau^{(k)}_m$, and we assume that it is uniformly distributed over [0,T_f]. We have $E[mui^{(k)}_p] = 0$ because the multipath gain $\alpha^{(k)}_m$ can be positive or negative with equal probability. Variance of $mui^{(k)}_p(\tau^{(k)})$ is given by

$$\begin{aligned} \sigma^2_{mui^{(k)}_p} &= E\left[mui^{(k)2}_p\right] - E\left[mui^{(k)}_p\right]^2 \\ &= E\left[\frac{1}{T_f} \int_0^{T_f} \left(\sqrt{E^{(k)}_{RX}} \int_0^{2T_p} \sum_{m=1}^{M^{(k)}} \alpha^{(k)}_m p(t - \tau^{(k)}_m - \tau^{(k)}) v(t) dt \right)^2 d\tau^{(k)} \right] \\ &= \frac{E^{(k)}_{RX}}{T_f} E\left[\int_0^{T_f} \left(\int_0^{2T_p} \sum_{m=1}^{M^{(k)}} \alpha^{(k)}_m p(t - \tau^{(k)}_m - \tau^{(k)}) v(t) dt \right)^2 d\tau^{(k)} \right] \end{aligned} \tag{4.18}$$

As all the delays $\tau^{(k)}$, amplitude of multi-paths $\alpha_m^{(k)}$ and delays of multi-paths $\tau_m^{(k)}$ are identically distributed for $k = 2, 3, \ldots, N$, we have

$$\begin{aligned}
&\sigma^2_{mui,l} = Var[Z_{mui,l}] \\
&= \sum_{k=2}^{N} \sum_{j=0}^{N_s-1} \sigma^2_{mui_p^{(k)}} \\
&= \sum_{k=2}^{N} \frac{N_s E_{RX}^{(k)}}{T_f} E\left[\int_0^{T_f} \left(\int_0^{2T_p} \sum_{m=1}^{M^{(k)}} \alpha_m^{(k)} p(t - \tau_m^{(k)} - \tau^{(k)}) v(t) dt \right)^2 d\tau^{(k)} \right] \\
&= \sum_{k=2}^{N} \frac{N_s E_{RX}^{(k)}}{T_f} E\left[\int_0^{T_f} \left(\int_0^{2T_p} \sum_{m=1}^{M} \alpha_m p(t - \tau_m - \tau) v(t) dt \right)^2 d\tau \right] \\
&= \frac{N_s}{T_f} E\left[\int_0^{T_f} \left(\int_0^{2T_p} \sum_{m=1}^{M} \alpha_m p(t - \tau_m - \tau) v(t) dt \right)^2 d\tau \right] \sum_{k=2}^{N} E_{RX}^{(k)} \\
&= \frac{N_s}{T_f} \sigma_M^2 \sum_{k=2}^{N} E_{RX}^{(k)}
\end{aligned} \tag{4.19}$$

where

$$\sigma_M^2 = E\left[\int_0^{T_f} \left(\int_0^{2T_p} \sum_{m=1}^{M} \alpha_m p(t - \tau_m - \tau) v(t) dt \right)^2 d\tau \right] \tag{4.20}$$

We then employ Maximal-Ratio Combing (MRC) to combine the contributions from the Rake fingers and obtain the decision variable

$$\begin{aligned}
Z &= \sum_{l=0}^{L-1} \sqrt{E_{RX}^{(1)}} \alpha_l Z_l \\
&= Z_u + Z_{mui} + Z_n
\end{aligned} \tag{4.21}$$

where

$$Z_u = \sum_{l=0}^{L-1} N_s E_{RX}^{(1)} \alpha_l^2 \tag{4.22}$$

$$Z_{mui} = \sum_{l=0}^{L-1} \sqrt{E_{RX}^{(1)}} \alpha_l Z_{mui,l} \tag{4.23}$$

$$Z_n = \sum_{l=0}^{L-1} \sqrt{E_{RX}^{(1)}} \alpha_l Z_{n,l} \tag{4.24}$$

The variance of MUI and noise, given that the channel condition is known, are given by

$$\begin{aligned} & Var[Z_{mui}|\alpha_l] \\ &= E_{RX}^{(1)} Var[\sum_{l=0}^{L-1} \alpha_l Z_{mui,l}] \\ &= E_{RX}^{(1)} \sum_{l=0}^{L-1} \alpha_l^2 Var[Z_{mui,l}] \\ &= \frac{N_s E_{RX}^{(1)}}{T_f} \sigma_M^2 \sum_{l=0}^{L-1} \alpha_l^2 \sum_{k=2}^{N} E_{RX}^{(k)} \end{aligned} \tag{4.25}$$

and

$$\begin{aligned} & Var[Z_n|\alpha_l] \\ &= E_{RX}^{(1)} Var[\sum_{l=0}^{L-1} \alpha_l Z_{n,l}] \\ &= E_{RX}^{(1)} \sum_{l=0}^{L-1} \alpha_l^2 Var[Z_{n,l}] \\ &= N_s E_{RX}^{(1)} N_0 \sum_{l=0}^{L-1} \alpha_l^2 \end{aligned} \tag{4.26}$$

The signal-to-noise ratio (SNR) and signal-to-interference ratio (SIR) are given by

$$SNR = \frac{(E[Z_u|\alpha_l])^2}{Var[Z_n|\alpha_l]} = \frac{(N_s E_{RX}^{(1)} \sum_{l=0}^{L-1} \alpha_l^2)^2}{N_s E_{RX}^{(1)} N_0 \sum_{l=0}^{L-1} \alpha_l^2} = \frac{E_b^{(1)} \sum_{l=0}^{L-1} \alpha_l^2}{N_0} \tag{4.27}$$

and

$$SIR = \frac{(E[Z_u|\alpha_l])^2}{Var[Z_{mui}|\alpha_l]} = \frac{(N_s E_{RX}^{(1)} \sum_{l=0}^{L-1} \alpha_l^2)^2}{\frac{N_s E_{RX}^{(1)}}{T_f} \sigma_M^2 \sum_{l=0}^{L-1} \alpha_l^2 \sum_{k=2}^{N} E_{RX}^{(k)}} = \frac{\sum_{l=0}^{L-1} \alpha_l^2}{\sigma_M^2 R_b \sum_{k=2}^{N} \frac{E_{RX}^{(k)}}{E_{RX}^{(1)}}} \tag{4.28}$$

where $R_b = 1/T_b = 1/(N_s T_f)$ is the data rate and $E_b^{(1)} = N_s E_{RX}^{(1)}$ is the received energy per bit from transmitter 1.

4.5 BER in the presence of AWGN & MUI

We employ the following decision rule for detection: if $Z > 0$, we decide that "0" is sent, otherwise "1" is sent. As the source symbols equal to "0" or "1" with equal

probability, the probability of error is: P{error}=0.5P{error|"0" is sent}+0.5P{error|"1" is sent}=P{Z<0 | "0" is sent}

Thus, we have

$$\begin{aligned}
&P\{error|\alpha_l\} \\
&= \mathrm{Q}\left(\sqrt{\frac{(E[Z|\alpha_l])^2}{Var[Z|\alpha_l]}}\right) \\
&= \mathrm{Q}\left(\sqrt{\frac{(E[Z_u|\alpha_l])^2}{Var[Z_n|\alpha_l]+Var[Z_{mui}|\alpha_l]}}\right) \\
&= Q\left(\sqrt{\left(\left(\frac{(E[Z_u|\alpha_l])^2}{Var[Z_n|\alpha_l]}\right)^{-1}+\left(\frac{(E[Z_u|\alpha_l])^2}{Var[Z_{mui}|\alpha_l]}\right)^{-1}\right)^{-1}}\right) \\
&= Q\left(\sqrt{\left(\left(\frac{E_b^{(1)}\sum_{l=0}^{L-1}\alpha_l^2}{N_0}\right)^{-1}+\left(\frac{\sum_{l=0}^{L-1}\alpha_l^2}{\sigma_M^2 R_b \sum_{k=2}^{N}\frac{E_{RX}^{(k)}}{E_{RX}^{(1)}}}\right)^{-1}\right)^{-1}}\right)
\end{aligned} \tag{4.29}$$

4.6 Rake Receivers

Three kinds of Rake receivers, namely All Rake (ARake), Selective Rake (SRake) and Partial Rake (PRake), are used in our work. ARake refers to the Rake receiver that has unlimited resources (taps or correlators) and instant adaptability, so that it can combine all the resolved multipath components in principle [8]. SRake selects the best L_s resolved multipath components (i.e. the components with the largest received amplitudes) available at the receiver output and PRake selects the first arriving L_p resolved multipath components. As a result, ARake has the best performance, while PRake has the worst. However, the good performance of ARake comes at a cost of high complexity and the large amount of resources required. Moreover, it should be noted that the performance gap between SRake and PRake reduces when the best few multipath components arrive early at the receiver, which is commonly observed in Line of Sight (LOS) scenarios.

Using the following sets of parameters, the BER vs. transmit SNR curves for different numbers of interferers using the above three types of Rake receivers are plotted in Fig. 4.6 and 4.7 after running 1000 iterations

- Data rate = 0.1Mbps.
- Transmit power: the transmit power of all the transmitters is controlled such that their received power at the intended receiver is the same.
- Number of Rake fingers for SRake and PRake: $L_s = 4$ and $L_p = 4$.
- Reference gain at a 1m: $c_0 = 10^{-4.7}$ and path loss exponent $\gamma = 1.7$ for multi-path-affected channels with LOS over short distances [27].
- Received pulse $p(t) = [1 - 4\pi(t/t_n)]\,[\exp(-2\pi(t/t_n)^2)]$ with $t_n = 0.7531ns$ and pulse width $T_p = 2ns$. In our analysis in the previous section, we are actually considering the pulse $p(t - T_p/2)$, so that it is defined in $[0, T_p]$.

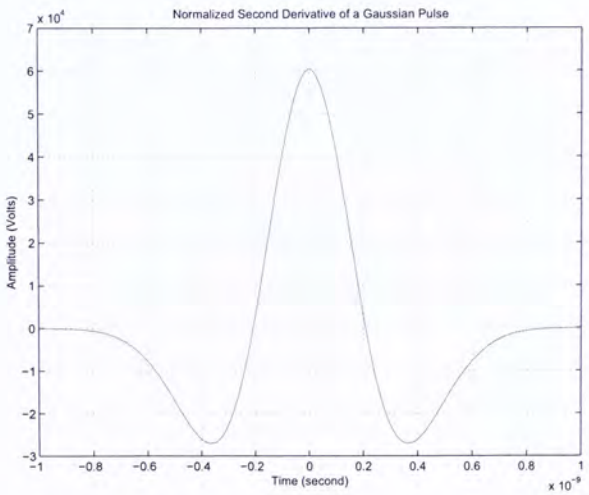

Figure 4.5: Normalized second derivative of the Gaussian Pulse: $p(t) = \left[1 - 4\pi\left(\frac{t}{t_n}\right)^2\right] \exp\left[-2\pi\left(\frac{t}{t_n}\right)^2\right]$ with $t_n = 0.7531ns$ and pulse width $T_p = 2ns$.

As shown in Fig. 4.7, when the number of interferers is large, the probability of error of PRake reaches the BER floor that its value cannot be further decreased by increasing the transmit power.

In these figures, we have eliminated the effect of path loss and shadowing and assume that ARake captures all the transmitted energy.

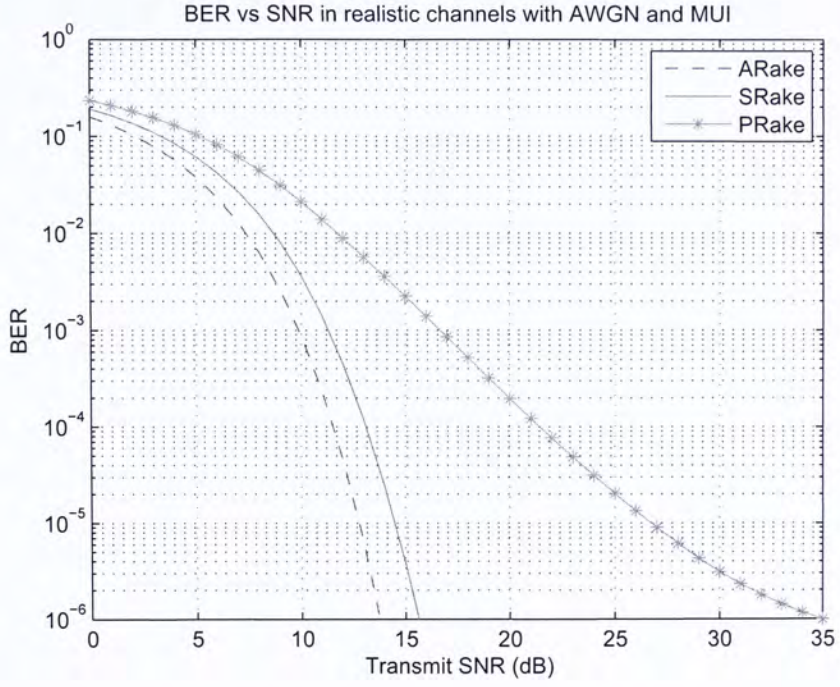

Figure 4.6: BER vs. transmit SNR for Rake receivers with 5 interferers.

4.7 Comparison of Simple Routing Algorithms in 1D Network

Consider a 1-D network with 5 nodes. They are separated with their neighbours by 1m as seen in Fig. 4.8. Suppose we want to transmit some information from node A to node E. Given an end-to-end BER requirement, which of the following strategies requires the minimum amount of transmit energy?

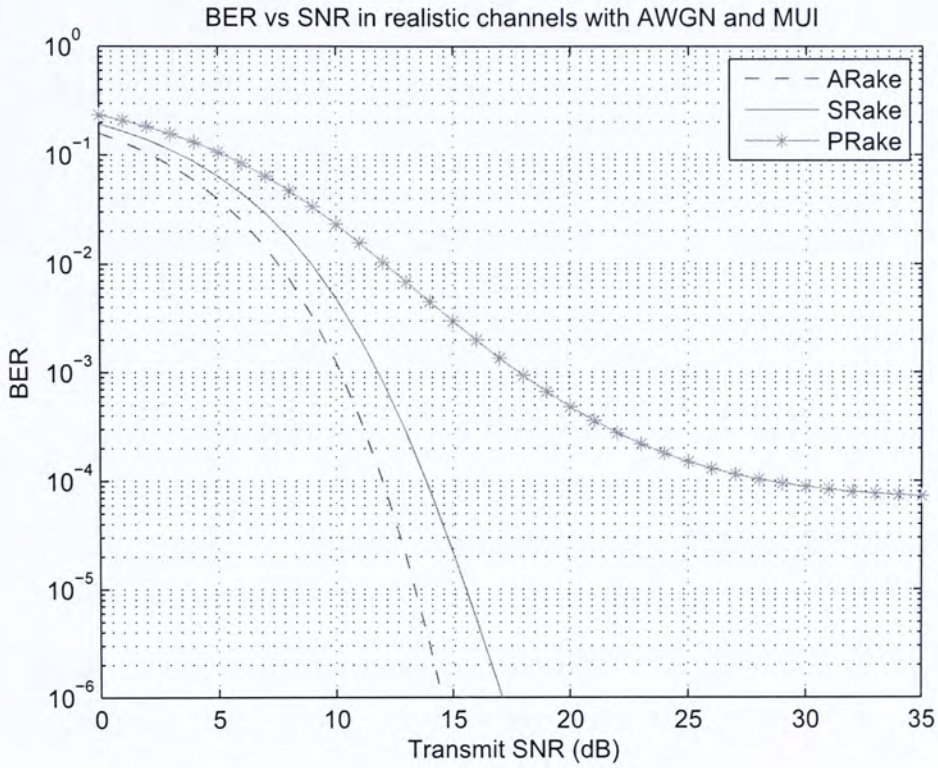

Figure 4.7: BER vs. transmit SNR for Rake receivers with 20 interferers.

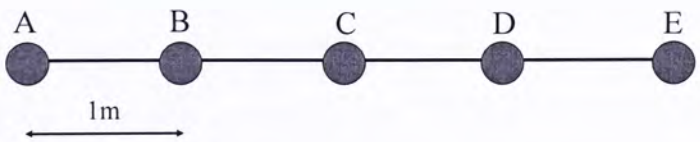

Figure 4.8: A 1D linear network with 5 nodes.

1. $A \rightarrow E$ (one hop)
2. $A \rightarrow C \rightarrow E$ (two hops)
3. $A \rightarrow B \rightarrow C \rightarrow D \rightarrow E$ (four hops)

We plot the BER vs. transmit SNR curves for transmission distance of 1m, 2m and 4m for LOS transmission using a realistic UWB channel model. The effects of multipath fading, shadowing and path loss are included. The parameters used in our simulations are as follows:

- Number of Rake fingers for SRake and PRake: $L_s = 3$ and $L_p = 3$.
- Reference gain at a 1m: $c_0 = 10^{-4.7}$ and path loss exponent $\gamma = 1.7$ for multipath-affected channels with LOS over short distances [27].
- Received pulse $p(t) = [1 - 4\pi(t/t_n)]\,[\exp(-2\pi(t/t_n)^2)]$ with $t_n = 0.7531ns$ and pulse width $T_p = 2ns$.

Assuming that there is no MUI for this network, the BER given that the channel gains for received multipath components are known is given by

$$P\{error|\alpha_l\} = Q\left(\sqrt{\frac{E_b^{(1)} \sum_{l=0}^{L-1} \alpha_l^2}{N_0}}\right) \tag{4.30}$$

After running 5000 simulations for different channel realizations, the results are shown in Fig. 4.10 to Fig. 4.12.

We now refer to Fig. 4.9. Let p be the BER for each hop.

- For scheme 1 with only one hop, the end-to-end probability of error from node A to E = p.
- For scheme 2, the end-to-end probability of error from node A to E = $2p(1-p) \approx 2p$, which the approximation is accurate when p is small.

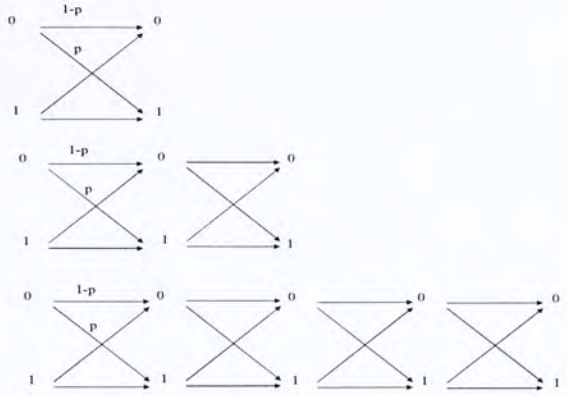

Figure 4.9: Per-hop and end-to-end BER for cases with 1, 2 and 4 hops.

- For scheme 3, the end-to-end probability of error from node A to E = $C_1^4 p(1-p)^3 + C_3^4 p^3(1-p) \approx 4p$, when p is small.

Consider the use of SRake as the receiver. Firstly, we evaluate the energy consumption of the three schemes when the end-to-end BER requirement is fixed to be 1×10^{-3}.

- Scheme 1: by reading Fig. 4.12 for 4m transmission and BER at 1×10^{-3}, total transmit SNR = 71.5dB = 1.41×10^7.
- Scheme 2: by reading Fig. 4.11 for 2m transmission and BER at $0.5 \times 10^{-3} = 5 \times 10^{-4}$, total transmit SNR = 2(67dB) = 1×10^7.
- Scheme 3: by reading Fig. 4.10 for 1m transmission and BER at $0.25 \times 10^{-3} = 2.5 \times 10^{-4}$, total transmit SNR = 4(62dB) = 6.34×10^6.

From the result above, we conclude that scheme 3 consumes the minimum amount of energy at end-to-end BER = 1×10^{-3} for SRake.

Next, we find the end-to-end BER when the end-to-end transmit SNR is fixed at 70dB:

- Scheme 1: by reading Fig. 4.12 for 4m transmission and per-hop SNR at 70dB, the end-to-end BER = 2.5×10^{-3}.
- Scheme 2: by reading Fig. 4.11 for 2m transmission and per-hop SNR at 0.5(70dB) = 67dB, the end-to-end BER = $2(5 \times 10^{-4}) = 1 \times 10^{-3}$.
- Scheme 3: by reading Fig. 4.10 for 1m transmission and per-hop SNR at 0.25(70dB) = 64dB, the end-to-end BER = $4(1.5 \times 10^{-4}) = 6 \times 10^{-4}$.

From the result above, we see that scheme 3 has the minimum end-to-end BER given a fixed end-to-end transmit SNR at 70dB for SRake.

□ **End of chapter.**

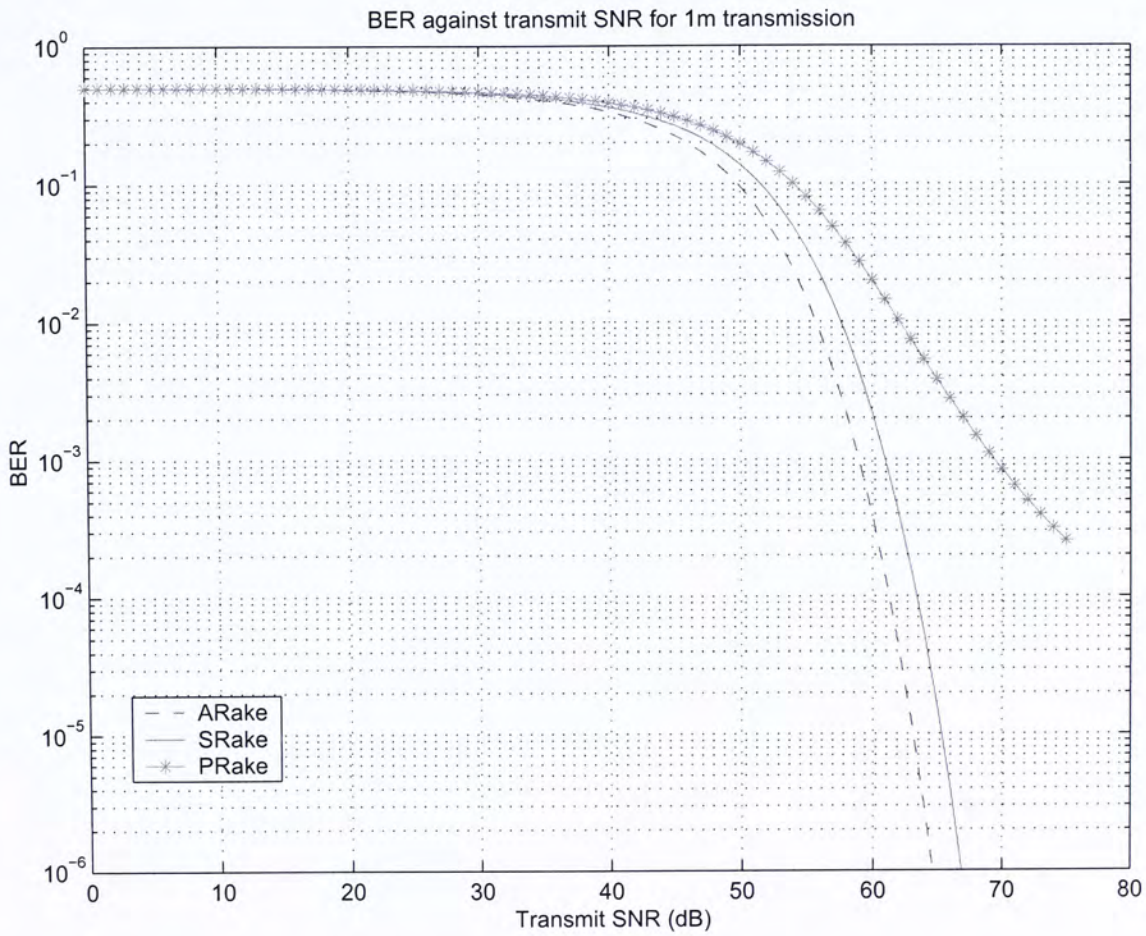

Figure 4.10: BER vs. transmit SNR curve for 1m transmission.

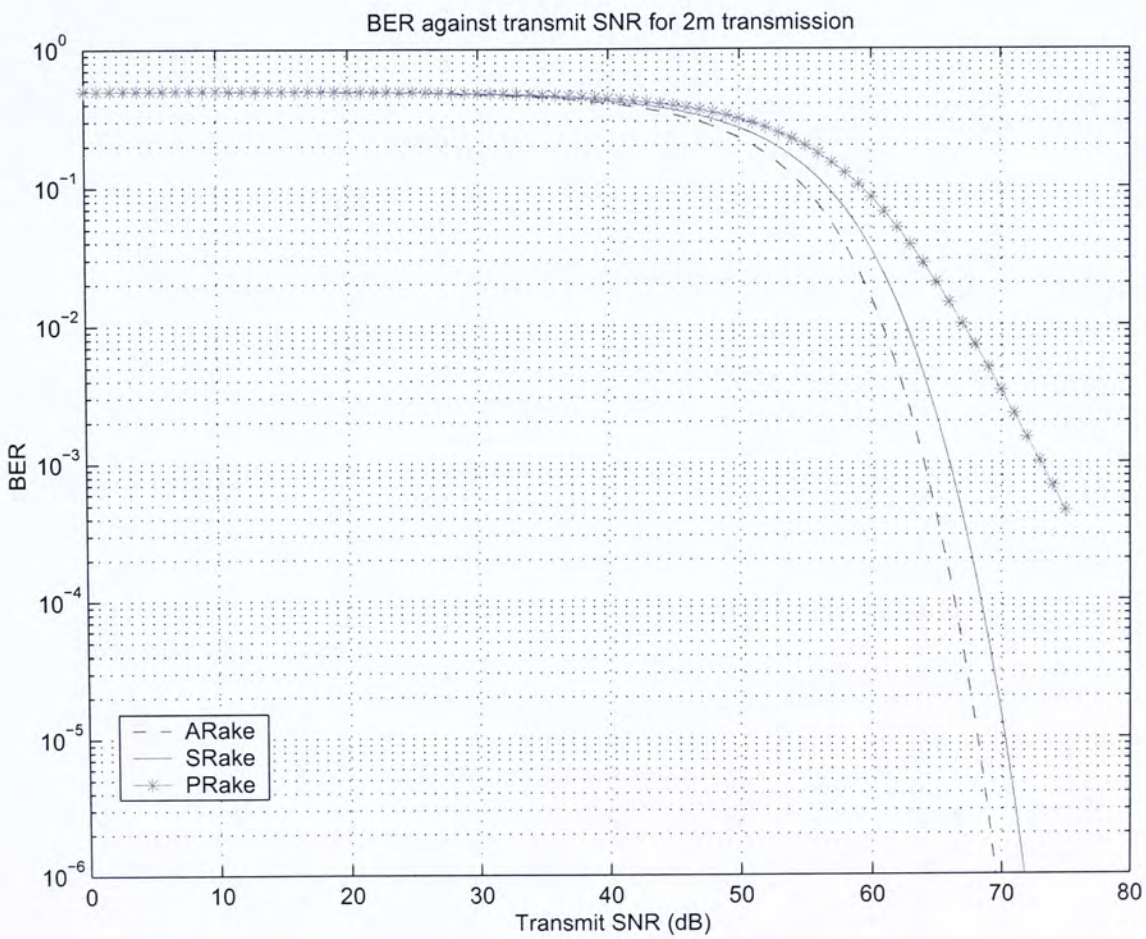

Figure 4.11: BER vs. transmit SNR curve for 2m transmission.

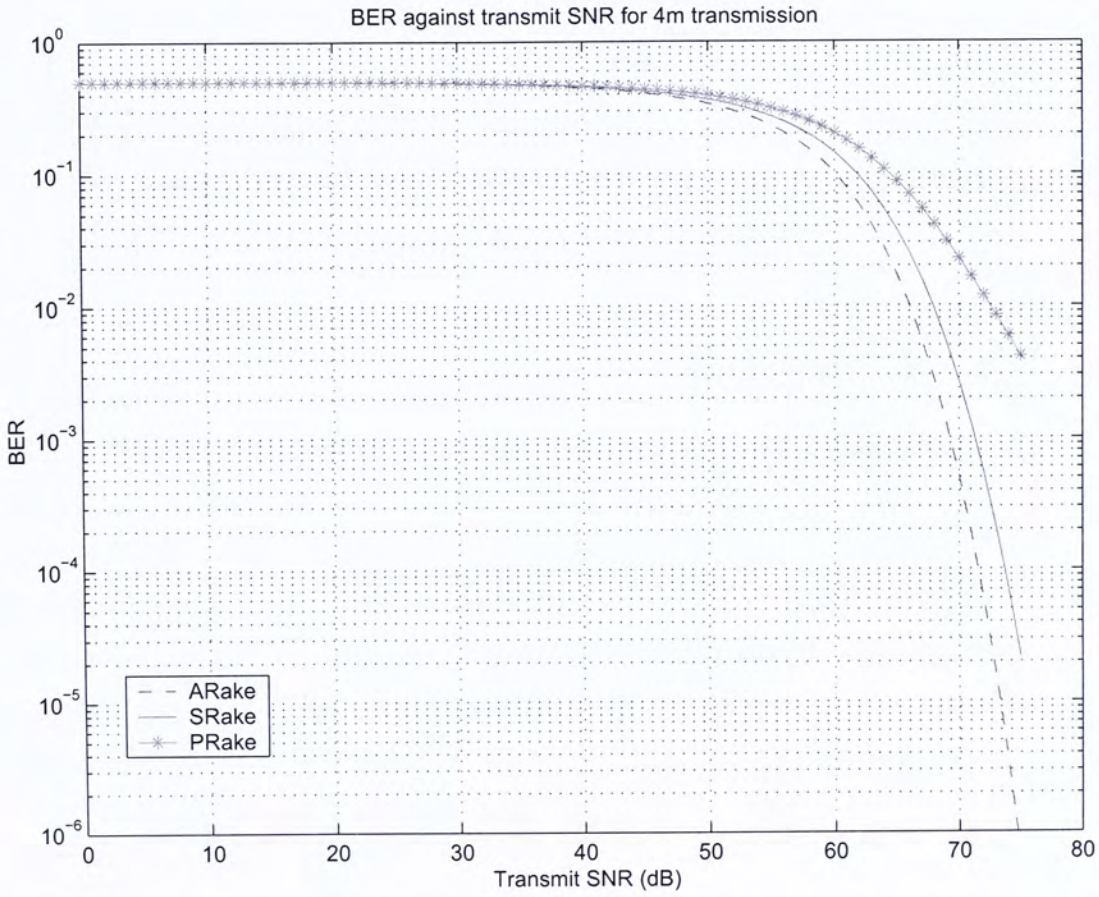

Figure 4.12: BER vs. transmit SNR curve for 4m transmission.

Chapter 5

Interference-Aware Routing in UWB Wireless Networks

In wireless ad hoc networks, limited power supply is the prime issue that we need to address. Moreover, because there are some nodes transmitting in the environment, we need to take into account the effect of the Multi-User Interference (MUI). In this chapter, we study interference-aware routing. We derive a suitable link cost for energy-efficient routing in UWB networks based on the BER expression derived in chapter 4. With this link cost, we introduce an Optimal Interference-Aware Routing Algorithm, which is capable of routing data packets from source to destination, using minimum energy per bit and at the same time achieving the end-to-end BER requirement. A Simple Interference-Aware Routing Algorithm is also introduced. The content in this chapter has published in [10].

5.1 Problem Formulation

We consider a wireless network with N nodes, which uses Impulse Radio (IR) UWB as the underlying physical layer technology. Each node is capable of transmitting using binary Pulse Position Modulation(PPM) - Time Hopping(TH) - UWB and receiving using L-finger Rake receiver. We assume that each node can transmit to

multiple nodes or receive from multiple nodes at the same time. However, simultaneous transmission and reception at a node is not allowed. At any time instant, a subset of the N nodes are transmitting, which appears to be interferers to some other nodes. For easy implementation of the hardware in the nodes, we assume that the transmit power level of each node is fixed.

Now, consider the case that a source S is going to send data packets to a sink T with a BER requirement ζ (i.e.$BER \leq \zeta$). For the intermediate nodes between the S and T, they will just buffer up the data bits and send them out until a whole packet has been received. In this way, we are considering the transmission of discrete data packets, rather than continuous flow of data streams in the network. We are interested to find a route from the source and sink, which has the minimum transmit energy per bit and at the same time achieves the BER requirement.

5.2 Optimal Interference-Aware Routing

5.2.1 Link Cost

We aim to minimize the transmit energy per bit $E_b = N_s E^{(1)}$, where $E^{(1)}$ is the energy for each transmitted pulse for user 1. From (4.29), the BER expression for PPM-TH-UWB in the presence of AWGN and MUI given that the channel is known can be expressed in the form

$$\begin{aligned} & P\{error|\alpha_l\} \\ &= \mathrm{Q}\left(\sqrt{\frac{(E[Z_u|\alpha_l])^2}{Var[Z_n|\alpha_l]+Var[Z_{mui}|\alpha_l]}}\right) \\ &= \mathrm{Q}\left(\sqrt{\frac{N_s \sum_{l=0}^{L-1} \alpha_l^2}{\frac{N_0 [D^{(1)}]^\gamma}{E^{(1)} c_0} + \frac{\sigma_M^2}{T_f} \sum_{k=2}^{N} \frac{E_{RX}^{(k)}}{E_{RX}^{(1)}}}}\right) \end{aligned} \tag{5.1}$$

where $D^{(k)}$ is the distance between user k and the receiver. c_0 is the reference gain of the signal at 1m and γ is the path loss exponent. $E_{RX}^{(k)}$ is the received energy for

each transmitted pulse at the receiver and it is given by

$$E_{RX}^{(k)} = \frac{E^{(k)} c_0}{[D^{(k)}]^\gamma} \tag{5.2}$$

As we assume that the transmit power level is fixed, $E^{(1)}$ is also fixed. Thus minimizing N_s is equivalent to minimizing E_b. From (5.1), we notice that for $P\{error|\alpha_l\} \leq \zeta$, there exists a positive number λ such that

$$\frac{N_s \sum_{l=0}^{L-1} \alpha_l^2}{\frac{N_0 [D^{(1)}]^\gamma}{E^{(1)} c_0} + \frac{\sigma_M^2}{T_f} \sum_{k=2}^{N} \frac{E_{RX}^{(k)}}{E_{RX}^{(1)}}} \geq \lambda \tag{5.3}$$

To obtain the smallest value of N_s which satisfies (5.3), the denominator of on the left hand side in the above equation should be the minimized. So, we take the link cost to be

$$C = [D^{(1)}]^\gamma + m \sum_{k=2}^{N} \frac{E_{RX}^{(k)}}{E_{RX}^{(1)}} \tag{5.4}$$

where

$$m = \frac{c_0 \sigma_M^2 E^{(1)}}{N_0 T_f} \tag{5.5}$$

With the assumption that each node is sending pulses with the same energy, (5.4) can be simplified into

$$C = [D^{(1)}]^\gamma + m \sum_{k=2}^{N} \left(\frac{D^{(1)}}{D^{(k)}} \right)^\gamma \tag{5.6}$$

5.2.2 Per-Hop BER Requirement and Scaling Effect

Suppose the path from S to T consists of h hops and BER requirement ζ is small, then we need to ensure than for each hop

$$P\{error|\alpha_l\} \leq \zeta/h \tag{5.7}$$

so that the end-to-end BER requirement ζ between the source S and sink T can be achieved. When $\zeta = 1 \times 10^{-3}$ and let $x = \frac{N_s \sum_{l=0}^{L-1} \alpha_l^2}{\frac{N_0 [D^{(1)}]^\gamma}{E^{(1)} c_0} + \frac{\sigma_M^2}{T_f} \sum_{k=2}^{N} \frac{E_{RX}^{(k)}}{E_{RX}^{(1)}}}$, we notice that for each hop

$$\text{When } h = 1,\ Q(\sqrt{x}) \leq 10^{-3} \Rightarrow x \geq 9.5495 \tag{5.8}$$

$$\text{When } h = 2,\ Q(\sqrt{x}) \leq 10^{-3}/2 \Rightarrow x \geq 10.8276 \tag{5.9}$$

$$\text{When } h = 3,\ Q(\sqrt{x}) \leq 10^{-3}/3 \Rightarrow x \geq 11.5800 \tag{5.10}$$

From (5.8)-(5.10), we observe that the BER requirement for each hop in route with more hops is more stringent than that with fewer hops. More energy is then needed. As a result, the total route cost from the source to the destination should not be just the summation of the link cost for the hops along the route. Furthermore, it has to be multiplied by a scaling factor that is greater than one. The larger the number of hops, the larger the scaling factor is. As an example, consider the network shown in Fig 5.1, which the link cost for each hop is shown. The route cost for the route AB = 5, while that of ACB should be equal to $(2 + 3) \times (10.8276/9.5495) = 5.6692$, according to the values in (5.8)-(5.10) (i.e. the scaling factor = 1.1338).

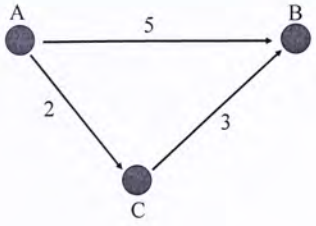

Figure 5.1: An example which shows the scaling effect of multihop routing.

5.2.3 Optimal Interference-Aware Routing

In view of the per-hop BER requirement and scaling effect of multihop routing as described in the previous section, it is not possible for us to find the route with the minimum route cost by simply applying Dijkstra's Algorithm. A variant of Dijkstra's Algorithm is used in our algorithm, which finds the shortest path with limited number of hops [31], to obtain the optimal route with the minimum transmit energy per bit in the network. The detail of the shortest path algorithm with a hop limit n is explained more explicitly as follows:

We consider a graph $\mathcal{G} = (\mathcal{V}, \mathcal{E})$, where $\mathcal{V}$ is the set of vertices and $\mathcal{E}$ is the set of edges. Let s be the source node, t be the sink node and n be the maximum number of hops. Define $dist_i(s, v)$ be the distance of the currently shortest path from s to v with at most i hops, $dist(a, b)$ be the distance between nodes a and b. Also, let $P_i(v)$ be the parent of vertex v on the currently shortest path from s to v with at most i hops. Let S_i be the set of vertices to which the shortest path with exactly i hops has been found. Let R be the set of all pairs (v, i) such that $dist_i(s, v) < \infty$ and that vertex v can be reached from source s in exactly i hops.

1. Input $\mathcal{G}$, s, t and n

   Initialization:

2. **for** all neighbour v of s **do** include $(v, 1)$ into R; **for** $i = 1$ to n **do** include s into S_i;

3. **for** vertex v, which is not s and not the neighbour of s **do**

4. **for** $i = 1$ to n **do** $dist_i(s, v) = \infty$;

5. **for** vertex v that is neighbour of s **do**

6. **for** $i = 1$ to n **do**

7. $dist_i(s,v) = dist(s,v)$ and $P_i(v) = s$;

Main Body:

8. **While** set R is non-empty **do**
9. **begin**
10. find (v,i) in set R which satisfies:
11. a) $dist_i(s,v) \leq dist_j(s,w)$ for all (w,j) in set R (i.e. to find (v,i) with the smallest value of $dist_i(s,v)$.) OR
12. b) $dist_i(s,v) = dist_j(s,w)$ for all (w,j) in set R and $i \leq j$; (i.e. if there are two elements which have the same smallest value of $dist_i(s,v)$, choose the one with a smaller number of hops.)
13. Include v into set S_i and exclude (v,i) from set R;
14. **if** $i < n$ **then**
15. **for** node w which is a neighbour of v and is not in S_{i+1} **do**
16. **begin**
17. **if** $dist_{i+1}(s,w) > dist_i(s,v) + dist(v,w)$, **then**
18. include $(w, i+1)$ into R;
19. **for** $j = i+1$ to n **do**
20. **if** $dist_j(s,w) > dist_{j-1}(s,v) + dist(v,w)$, **then**
21. $dist_j(s,w) = dist_{j-1}(s,v) + dist(v,w)$ and $P_j(w) = v$;
22. **end**
23. **end**

24. $path = t$; $v = t$, $i = n$;

25. **repeat**

26. $v = P_i(v)$;

27. $path = v \oplus path$;

28. $i = i - 1$;

29. **until** v = s.

After executing the algorithm, *path* is the shortest path with at most n hops.

Then using the algorithm above, our Optimal Interference-aware Routing Algorithm is suggested as follows:

1. Calculate the link cost for every hops in the network according to (5.4);
2. Run the traditional Dijkstra's Algorithm;
3. Obtain the path p, number of hops h and route cost m (= sum of link cost × scaling factor);
4. Set $minpath = p$, $minhop = h$ and $mincost = m$;
5. **While** $(h > 1)$ **do**
6. Run shortest path algorithm with at most $h - 1$ hops; [31]
7. Obtain the new route: path p', number of hop h' and route cost m';
8. **If** $(m' < mincost)$ **then**
9. $minpath = p'$, $minhop = h'$ and $mincost = m'$;
10. **else if** $(m' = mincost)$ and $(h' < minhop)$ **then**
11. $minpath = p'$, $minhop = h'$ and $mincost = m'$;
12. $h = h'$;

13. **end**

After running this algorithm, the optimal path is *minpath*.

Steps 1 to 4 form a route by applying traditional Dijkstra's algorithm to the link costs obtained. Steps 5 to 13 tries to find a route with a lower route cost by searching for routes with smaller number of hops. It is possible because a route with a smaller number of hops has a smaller scaling factor. Searching for a route with a larger number of hops is fruitless, not only because of the larger scaling factor, but also due to the fact that it is not possible to find a route with a smaller sum of link cost than the route obtained in steps 1 to 4. Step 10 chooses a route with a smaller number of hops when the route costs of two routes are equal. It is a desirable choice because the delay in transmission can be kept as small as possible.

5.3 Performance Evaluation

In this section, we evaluate the performance of interference-aware routing, based on the following parameters:

- Transmitter: PPM-TH-UWB is used as the signaling format.
- Transmit power for each node = 0.5mW.
- Receiver: Selective Rake, which captures the best four multipath components at the receiver input.
- Received pulse $p(t) = [1 - 4\pi(t/t_n)]\,[\exp(-2\pi(t/t_n)^2)]$ with $t_n = 0.7531ns$ and pulse width $T_p = 2ns$.
- BER requirement $= 1 \times 10^{-3}$.
- Frame duration $T_f = 5ns$.
- $\sigma_M^2 = 4.55 \times 10^{-9}$.

- Reference gain at a 1m: $c_0 = 10^{-4.7}$ and path loss exponent $\gamma = 1.7$ for multipath-affected channels with Line of Sight (LOS) over short distances [27].
- Noise power spectral density $N_0 = 4 \times 10^{-20}$W/Hz.

We compare the energy consumption of the following five schemes using computer simulations:

- Optimal Interference-Aware Routing: We use the link cost in (5.4) and find out the shortest path using our Optimal Interference-aware Routing Algorithm.
- Simple Interference-Aware Routing: We use the link cost in (5.4) and find out the shortest path using the traditional Dijkstra's Algorithm only (i.e. running steps 1 to 4 of our Optimal Interference-Aware Routing Algorithm only).
- Long-Hop Routing: It aims to form a route using nodes which are far apart. In our simulation, we take it to be the one-hop routing, which the source directly sends the data packets to the sink without going through any relay nodes.
- Short-Hop Routing: It aims to form a route using nodes which are close together. The route is obtained by setting the link cost to be the distance between nodes to the power γ (=1.7) and running the traditional Dijkstra's Algorithm.
- Location-Based Routing: We use the Packet Transfer Protocol as described in [20]. In this protocol, a node forwards packets to a closest neighbor within its transmission range R, which is closer to the destination. (We take $R = 15$m in our simulation.) If the destination is within R, the node will send the packet directly to the destination.

Using a $30m \times 30m$ network with 40 nodes in random topology, we find out the transmit energy per bit required for each scheme. In our evaluation, since a node cannot send and receive at the same time, we assume that all the interferers cannot act as relay nodes. An example is shown in Fig. 5.2 to illustrate the five routing schemes in a typical scenario. There are 40 nodes in the network, where the 15 big

dots (nodes 1 to 15) in the figure are interferers, and the remaining 25 small dots (nodes 16 to 40) are the source, sink and potential relay nodes. Source is node 16 and sink is node 40. In this example, the five different routes and their transmit energy per bit E_b are:

- Optimal Interference-aware Routing: $16 \rightarrow 36 \rightarrow 18 \rightarrow 40$ ($E_b = 1.36nJ$)
- Simple Interference-aware Routing: $16 \rightarrow 36 \rightarrow 18 \rightarrow 33 \rightarrow 40$ ($E_b = 1.40nJ$)
- Long-Hop Routing: $16 \rightarrow 40$ ($E_b = 2.32nJ$)
- Short-Hop Routing: $16 \rightarrow 38 \rightarrow 35 \rightarrow 17 \rightarrow 33 \rightarrow 40$ ($E_b = 1.56nJ$)
- Location-based Routing: $16 \rightarrow 38 \rightarrow 36 \rightarrow 40$ ($E_b = 1.93nJ$)

We notice that scheme 1 finds a route which requires the minimum transmit energy per bit. Due to the scaling effect of multihops, it turn out that the optimal route in scheme 1 consists of one hop less than that in scheme 2.

To investigate the average performance, we run 1000 simulations for each level of interference, which is directly proportional to the number of active links or interferers in the system. The result is shown in Fig. 5.3. We observe that our interference-aware schemes consume 3dB less energy than long-hop, short-hop and location-based routing in many cases. While comparing the simple interference-aware routing with optimal interference-aware routing, we see that the latter one consumes a little less energy than the former one.

□ **End of chapter.**

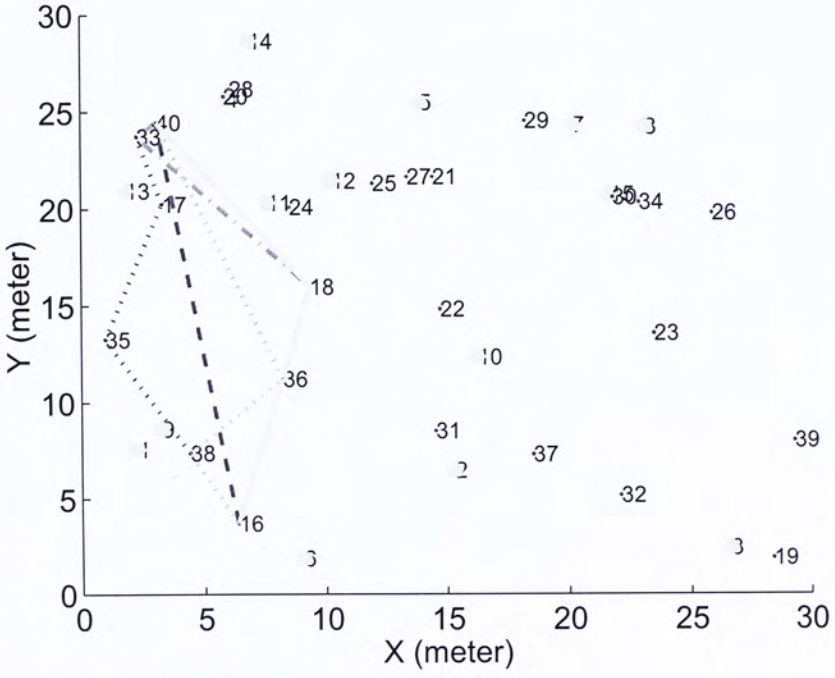

Figure 5.2: An example showing the output of the five routing schemes.

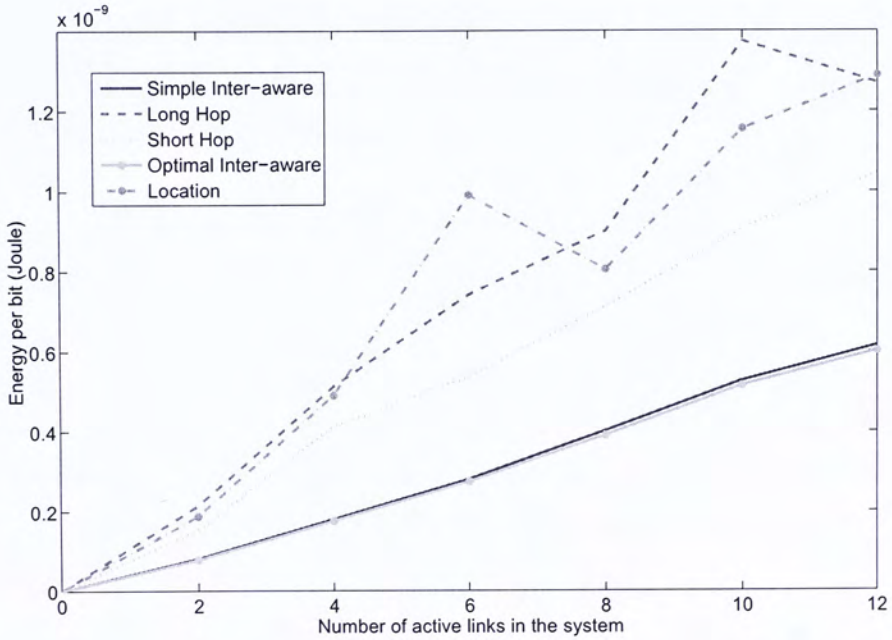

Figure 5.3: Energy consumption at different levels of interference for the five schemes.

Chapter 6

Cooperative Routing in UWB Wireless Networks

In this chapter, we consider cooperative routing using UWB physical layer model, and the setup is similar to that in chapter 3. The major differences are that MUI is considered here, but simple analytical result for the optimal power distribution ratio β as in Rayleigh fading channel is absent for PPM-TH-UWB. As a result, we modify the cooperative routing algorithm suggested in chapter 3, based on some analytical results and computer experiments for cooperative UWB. The content in this chapter has published in [11].

6.1 Two-Node Cooperative Communication

6.1.1 Received Signal for Non-Cooperative Communication

In Fig. 6.1, suppose source S uses node 1 as a relay to transmit data packets to sink T. We assume that node 1 transmits data to sink T with energy per pulse equals to E_T. Let nodes 3 to N be undesired users, which are continuously transmitting at the same power level as node 1, with energy per pulse equals to E_T. With reference to $s^{(k)}(t)$ in (4.1) and $h^{(k)}(t)$ in (4.3), we assume that there is a perfect synchronization

between transmitter 1 and the reference receiver, i.e. $\zeta^{(1)}$ is known by the receiver. The composite received signal at the output of the receiver's antenna is modeled as

$$r(t) = s^{(1)}(t) * h^{(1)}(t) + \sum_{k=3}^{N} s^{(k)}(t) * h^{(k)}(t) + n(t) \tag{6.1}$$

where $n(t)$ is a zero mean, AWGN random process with two-sided power spectral density $N_0/2$.

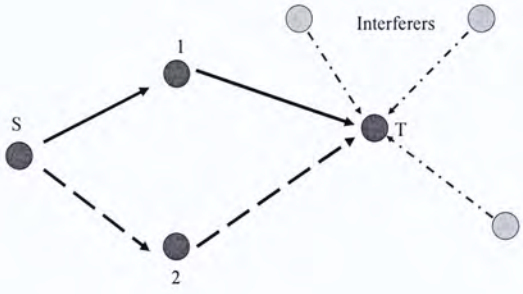

Figure 6.1: Non-Cooperative ($S \rightarrow 1 \rightarrow T$) vs. Cooperative Routing ($S \rightarrow \{1,2\} \rightarrow T$) in the presence of MUI.

6.1.2 Received Signal for Two-Node Cooperative Communication

As shown in Fig. 6.1, because of the broadcast nature of wireless communication, node 2 also receives the signal from S to node 1. As a result, node 2 can cooperate with node 1 and send to node T at the same time. We assume that transmit energy per pulse for node 1 and 2 are βE_T and $(1-\beta)E_T$ respectively, where $0 \leq \beta \leq 1$. That means the total transmit energy per pulse to node T remains E_T, but it is distributed between node 1 and 2 according to a certain ratio β. Nodes 3 to N

are still undesired users, which are continuously transmitting with energy per pulse equals to E_T. We assume that there is a perfect synchronization between transmitter i and the reference receiver, where $i = 1$ or 2. The composite received signal at the output of the receiver's antenna is modeled as

$$r(t) = \sum_{k=1}^{N} s^{(k)}(t) * h^{(k)}(t) + n(t) \tag{6.2}$$

6.1.3 Probability of Error

Based on (4.27), (4.28) and (4.29), we obtain

$$P\{error|\alpha_l\} = Q\left(\sqrt{SINR}\right) \tag{6.3}$$

where the inverse of signal-to-interference and noise ratio (SINR) is given by

$$1/\text{SINR} = 1/\text{SNR} + 1/\text{SIR} \tag{6.4}$$

No Cooperation

For the case without cooperation, as discussed in section 6.1.1 and with reference to (4.27) and (4.28), because that there are only $N-1$ transmissions, with user 1 being the intended transmitter and users 3 to N being the undesired users, the signal-to-noise ratio (SNR) and signal-to-interference ratio (SIR) are

$$\begin{aligned} SNR &= \frac{N_s E_{RX}^{(1)} \sum_{l=0}^{L-1} \alpha_l^{(1)2}}{N_0} \\ SIR &= \frac{E_{RX}^{(1)} \sum_{l=0}^{L-1} \alpha_l^{(1)2}}{R_b \sigma_M^2 \sum_{k=3}^{N} E_{RX}^{(k)}} \end{aligned} \tag{6.5}$$

where $\alpha_l^{(k)}$ is the amplitude of a multipath component detected by the lth finger of the Rake receiver when the transmitter is node k. R_b is the data rate. σ_M^2 is a variable that depends on pulse shape and the value of T_f. $Q(x)$ is defined as

the probability that a standard normal random variable (zero mean, unit variance) exceeds x. $E_{RX}^{(k)}$ is the received energy for each transmitted pulse at the receiver and it is given by

$$E_{RX}^{(k)} = \frac{E^{(k)} c_0}{[D^{(k)}]^{\gamma}} \tag{6.6}$$

where $E^{(k)}$ is the transmit energy per pulse for node k and $D^{(k)}$ is the distance between node k and the receiver. c_0 is the reference gain at a 1m and γ is the path loss exponent.

Simple Cooperation

For the case with cooperation, we refer to the discussion in section 6.1.2. We employ two Rake receivers to detect the signals from user 1 and user 2. Each of the Rake receivers is intended to capture the signal contribution from one user and treat the signal from other users as interference. Define $E_{RX}^{(k)} = (A^{(k)} X^{(k)})^2$

For the 1st Rake, the decision variable for finger l is

$$Z_l^{(1)} = Z_{u,l}^{(1)} + Z_{mui,l}^{(1)} + Z_{n,l}^{(1)} \tag{6.7}$$

where $Z_{u,l}^{(1)} = \sqrt{E_{RX}^{(1)}} N_s \alpha_l^{(1)}$, $Var[Z_{mui,l}^{(1)}] = \frac{N_s}{T_f} \sigma_M^2 \sum_{k=2}^{N} E_{RX}^{(k)}$, $Var[Z_{n,l}^{(1)}] = N_s N_0$, with reference to (4.13), (4.19) and (4.15).

For the 2nd Rake, the decision variable for finger l is

$$Z_l^{(2)} = Z_{u,l}^{(2} + Z_{mui,l}^{(2)} + Z_{n,l}^{(2)} \tag{6.8}$$

where $Z_{u,l}^{(2)} = \sqrt{E_{RX}^{(2)}} N_s \alpha_l^{(2)}$, $Var[Z_{mui,l}^{(2)}] = \frac{N_s}{T_f} \sigma_M^2 \sum_{k=1,k\neq 2}^{N} E_{RX}^{(k)}$, $Var[Z_{n,l}^{(2)}] = N_s N_0$, with reference also to (4.13), (4.19) and (4.15).

Employing MRC to obtain the decision variable

$$\begin{aligned} Z &= \sum_{l=0}^{L-1} (\sqrt{E_{RX}^{(1)}} \alpha_l^{(1)} Z_l^{(1)} + \sqrt{E_{RX}^{(2)}} \alpha_l^{(2)} Z_l^{(2)}) \\ &= Z_u + Z_{mui} + Z_n \end{aligned} \tag{6.9}$$

where

$$Z_u = \sum_{l=0}^{L-1} (\sqrt{E_{RX}^{(1)}} \alpha_l^{(1)} Z_{u,l}^{(1)} + \sqrt{E_{RX}^{(2)}} \alpha_l^{(2)} Z_{u,l}^{(2)}) \tag{6.10}$$

and

$$Z_{mui} = \sum_{l=0}^{L-1} (\sqrt{E_{RX}^{(1)}} \alpha_l^{(1)} Z_{mui,l}^{(1)} + \sqrt{E_{RX}^{(2)}} \alpha_l^{(2)} Z_{mui,l}^{(2)}) \tag{6.11}$$

and

$$Z_n = \sum_{l=0}^{L-1} (\sqrt{E_{RX}^{(1)}} \alpha_l^{(1)} Z_{n,l}^{(1)} + \sqrt{E_{RX}^{(2)}} \alpha_l^{(2)} Z_{n,l}^{(2)}) \tag{6.12}$$

.

Then, we have

$$\begin{aligned} & E[Z|\alpha_l] = E[Z_u|\alpha_l] \\ & = N_s(E_{RX}^{(1)} \sum_{l=0}^{L-1} \alpha_l^{(1)2} + E_{RX}^{(2)} \sum_{l=0}^{L-1} \alpha_l^{(2)2}) \end{aligned} \tag{6.13}$$

and

$$\begin{aligned} & Var[Z_{mui}|\alpha_l] \\ & = \frac{N_s \sigma_M^2 E_{RX}^{(1)} \sum_{l=0}^{L-1} \alpha_l^{(1)2}}{T_f} \sum_{k=2}^{N} E_{RX}^{(k)} + \frac{N_s \sigma_M^2 E_{RX}^{(2)} \sum_{l=0}^{L-1} \alpha_l^{(2)2}}{T_f} \sum_{k=1,k\neq 2}^{N} E_{RX}^{(k)} \\ & = \frac{N_s \sigma_M^2}{T_f} \left(E_{RX}^{(1)} \sum_{l=0}^{L-1} \alpha_l^{(1)2} \sum_{k=2}^{N} E_{RX}^{(k)} + E_{RX}^{(2)} \sum_{l=0}^{L-1} \alpha_l^{(2)2} \sum_{k=1,k\neq 2}^{N} E_{RX}^{(k)} \right) \end{aligned} \tag{6.14}$$

and

$$\begin{aligned} & Var[Z_n|\alpha_l] \\ & = N_s E_{RX}^{(1)} N_0 \sum_{l=0}^{L-1} \alpha_l^{(1)2} + N_s E_{RX}^{(2)} N_0 \sum_{l=0}^{L-1} \alpha_l^{(2)2} \\ & = N_s N_0 \left(E_{RX}^{(1)} \sum_{l=0}^{L-1} \alpha_l^{(1)2} + E_{RX}^{(2)} \sum_{l=0}^{L-1} \alpha_l^{(2)2} \right) \end{aligned} \tag{6.15}$$

The SNR and SIR are

$$\begin{aligned} SNR &= \frac{(E[Z|\alpha_l])^2}{Var[Z_n|\alpha_l]} \\ &= \frac{N_s^2(E_{RX}^{(1)}\sum_{l=0}^{L-1}\alpha_l^{(1)2}+E_{RX}^{(2)}\sum_{l=0}^{L-1}\alpha_l^{(2)2})^2}{N_sN_0\left(E_{RX}^{(1)}\sum_{l=0}^{L-1}\alpha_l^{(1)2}+E_{RX}^{(2)}\sum_{l=0}^{L-1}\alpha_l^{(2)2}\right)} \\ &= \frac{N_s(E_{RX}^{(1)}\sum_{l=0}^{L-1}\alpha_l^{(1)2}+E_{RX}^{(2)}\sum_{l=0}^{L-1}\alpha_l^{(2)2})}{N_0} \end{aligned} \tag{6.16}$$

$$\begin{aligned} SIR &= \frac{(E[Z|\alpha_l])^2}{Var[Z_{mui}|\alpha_l]} \\ &= \frac{N_s^2(E_{RX}^{(1)}\sum_{l=0}^{L-1}\alpha_l^{(1)2}+E_{RX}^{(2)}\sum_{l=0}^{L-1}\alpha_l^{(2)2})^2}{\frac{N_s\sigma_M^2}{T_f}\left(E_{RX}^{(1)}\sum_{l=0}^{L-1}\alpha_l^{(1)2}\sum_{k=2}^{N}E_{RX}^{(k)}+E_{RX}^{(2)}\sum_{l=0}^{L-1}\alpha_l^{(2)2}\sum_{k=1,k\neq 2}^{N}E_{RX}^{(k)}\right)} \\ &= \frac{(E_{RX}^{(1)}\sum_{l=0}^{L-1}\alpha_l^{(1)2}+E_{RX}^{(2)}\sum_{l=0}^{L-1}\alpha_l^{(2)2})^2}{R_b\sigma_M^2\left(E_{RX}^{(1)}\sum_{l=0}^{L-1}\alpha_l^{(1)2}\sum_{k=2}^{N}E_{RX}^{(k)}+E_{RX}^{(2)}\sum_{l=0}^{L-1}\alpha_l^{(2)2}\sum_{k=1,k\neq 2}^{N}E_{RX}^{(k)}\right)} \end{aligned}$$

where $R_b = 1/(N_sT_f)$ is the data rate.

Cooperation with Interference Cancellation

For the case with interference cancellation, the expressions are the same as above, accept that

$$Var[Z_{mui,l}^{(1)}] = Var[Z_{mui,l}^{(2)}] = \frac{N_s}{T_f}\sigma_M^2\sum_{k=3}^{N}E_{RX}^{(k)} \tag{6.17}$$

because the mutual interferences between users 1 and 2 are removed. For the SNR, it is the same as that in (6.16). For the SIR, because

$$\begin{aligned} &Var[Z_{mui}|\alpha_l] \\ &= \sum_{l=0}^{L-1}Var\left[\sqrt{E_{RX}^{(1)}}\alpha_l^{(1)}Z_{mui,l}^{(1)}\right]+\sum_{l=0}^{L-1}Var\left[\sqrt{E_{RX}^{(2)}}\alpha_l^{(2)}Z_{mui,l}^{(2)}\right] \\ &= \sum_{l=0}^{L-1}E_{RX}^{(1)}\alpha_l^{(1)2}Var\left[Z_{mui,l}^{(1)}\right]+\sum_{l=0}^{L-1}E_{RX}^{(2)}\alpha_l^{(2)2}Var\left[Z_{mui,l}^{(2)}\right] \\ &= (E_{RX}^{(1)}\sum_{l=0}^{L-1}\alpha_l^{(1)2}+E_{RX}^{(2)}\sum_{l=0}^{L-1}\alpha_l^{(2)2})\frac{N_s\sigma_M^2}{T_f}\sum_{k=3}^{N}E_{RX}^{(k)} \end{aligned} \tag{6.18}$$

Thus, the SNR and SIR are

$$SNR = \frac{N_s(E_{RX}^{(1)} \sum_{l=0}^{L-1} \alpha_l^{(1)2} + E_{RX}^{(2)} \sum_{l=0}^{L-1} \alpha_l^{(2)2})}{N_0}$$

$$\begin{aligned} SIR &= \frac{(E[Z|\alpha_l])^2}{Var[Z_{mui}|\alpha_l]} \\ &= \frac{N_s^2(E_{RX}^{(1)} \sum_{l=0}^{L-1} \alpha_l^{(1)2} + E_{RX}^{(2)} \sum_{l=0}^{L-1} \alpha_l^{(2)2})^2}{(E_{RX}^{(1)} \sum_{l=0}^{L-1} \alpha_l^{(1)2} + E_{RX}^{(2)} \sum_{l=0}^{L-1} \alpha_l^{(2)2}) \frac{N_s \sigma_M^2}{T_f} \sum_{k=3}^{N} E_{RX}^{(k)}} \\ &= \frac{E_{RX}^{(1)} \sum_{l=0}^{L-1} \alpha_l^{(1)2} + E_{RX}^{(2)} \sum_{l=0}^{L-1} \alpha_l^{(2)2}}{R_b \sigma_M^2 \sum_{k=3}^{N} E_{RX}^{(k)}} \end{aligned} \tag{6.19}$$

Performance Evaluation

Using (6.3)-(6.19), we evaluate the above three transmission strategies. We define SNR_T to be the transmit SNR, with value equals to $N_s E_T/N_0$ and dist(A,B) to be the Euclidean distance between nodes A and B. We consider a system using Partial Rake receiver with three fingers, which captures the first three arriving multipath components. With dist(1,T) = dist(2,T) = 2m; dist(interferer,T) = 3m, number of interferers = 10; data rate R_b = 0.1Mbps, we obtain the graph in Fig. 6.2. We observe that there is a significant improvement in performance when cooperation is applied in a fading environment. Moreover, the curves for cooperation with and without interference cancellation overlap with each other, indicating a limited effect in additional interference due to the simultaneous transmissions of both nodes 1 and 2 during cooperation.

6.2 Problem Formulation

We consider a wireless network with a number of nodes, which some of them are interferers who are continuously transmitting. All the nodes, including the interferers, transmit at the same power level. The physical layer is supported by IR-UWB. Each

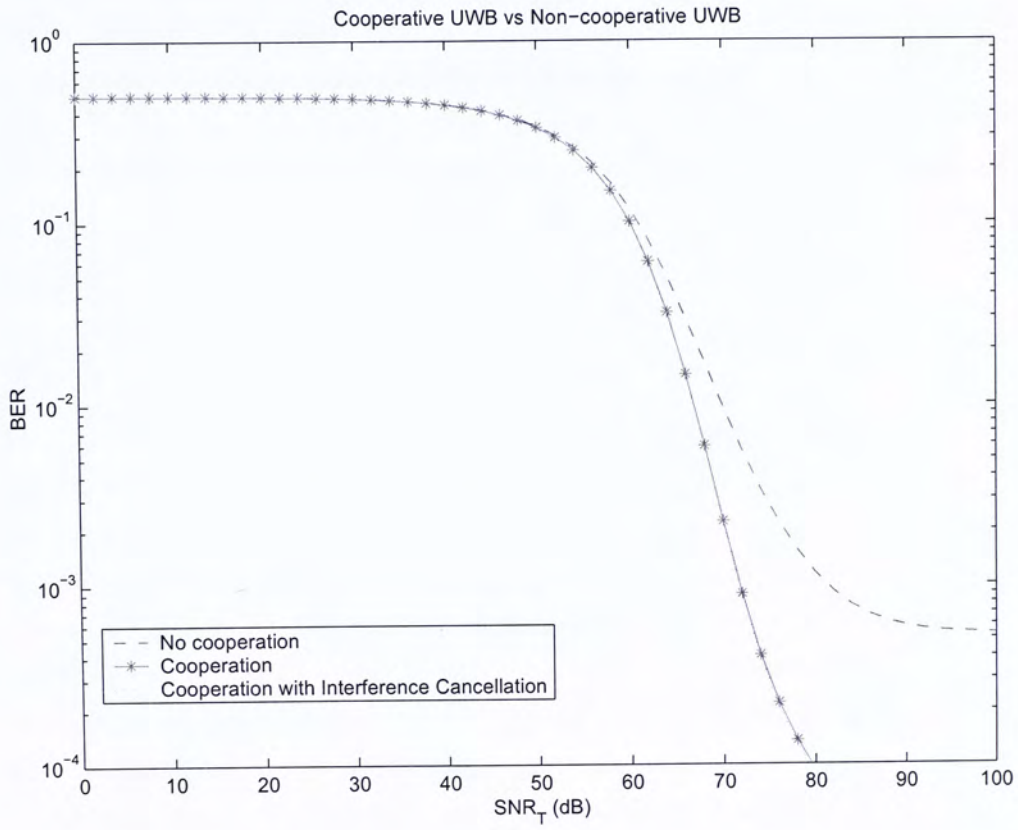

Figure 6.2: BER vs. SNR_T curve for the cases with and without cooperation.

node is capable of transmitting using binary PPM-TH-UWB and receiving using L-finger Partial Rake (PRake) receiver. PRake receiver has a low complexity as it combines the first L arriving multipath components. For the nodes, we assume that they cannot transmit or receive at the same time, but they are allowed to transmit at a variable power level. We assume that if a packet is received with SINR above a certain threshold, it is error-free.

Assume that we are given a single path route from the source to the sink, which can be generated by any routing algorithm. As cooperation helps combat the deleterious effect of fading, given the single path route, network topology and interference level, we are interested in finding a simple cooperative strategy that makes the system less susceptible to channel variations due to multipath fading.

6.3 Cooperative Routing Algorithm

Based on the discussion in section 6.1, as we see that the simple two-node cooperative scheme has a significant advantage over the non-cooperative one, we apply it to our Cooperative Routing Algorithm. There is only one sender and one receiver for each hop for the single path route initially. We now decide if any node, which has "overheard" the message in the previous hop, should cooperate with the original sender in this hop and transmit to the receiver. In this way, there will be two simultaneous transmissions to the receiver in each hop. We distribute the transmit power equally between the two senders, i.e. $\beta = 0.5$.

Actually, the algorithm below can be applied to any ad hoc networks in general, but we evaluate its performance in a UWB wireless network. In our algorithm, we use $\mathbf{C}(i, j)$ to denote the element in the ith row and jth column in matrix $\mathbf{C}$. The steps for our algorithm are as follows:

1. **(Input)** A single path route $\mathbf{S}$ is generated by a routing algorithm, e.g. $\mathbf{S}$ = [1 2 3 4], of which the numbers in the vector represent the node ID. We define l to be the number of elements in the single path route.

2. **(Initialization)** Initialize a cooperative route by creating a matrix **C** with dimension $2 \times l$, of which the upper row is identical to **S** and the lower row is filled with zeros. E.g. $C = \begin{pmatrix} 1 & 2 & 3 & 4 \\ 0 & 0 & 0 & 0 \end{pmatrix}$

3. **(Assignment)** For each iteration, we consider three consecutive nodes in **S** so that there are a total of $l-2$ iterations. For the kth iteration, define h_1=**C**(1,k); h_2=**C**(2,k); m=**C**(1,k+1); t=**C**(1,k+2). As seen in Fig. 6.3 and 6.4, the arrow(s) from h_1 (and h_2 if there is cooperative communication) to m represents the transmission in the previous hop that has taken place and the arrow from m to t represents the intended transmission in this hop. We are going to determine if there are any nodes that can overhear the signal in the previous hop should cooperate with m to send to t in this hop.

4. **(Identify nodes which can overhear the message)**

   a) Neglecting the effects of shadowing and multipath fading (i.e. assume $\sum_{l=0}^{L-1} \alpha_l^{(i)2} = 1$ for $i = 1$ and 2), calculate the minimum transmit energy per pulse from h_1 to m required by a packet to reach the SINR requirement at m according to (6.3)-(6.5). It is given by

$$E_T = \frac{[D^{(1)}]^\gamma N_0}{N_s c_0 \left[\frac{1}{SINR} - R_b \sigma_M^2 \sum_k \left(\frac{D^{(1)}}{D^{(k)}}\right)^\gamma\right]} \tag{6.20}$$

   where k is the index of the interferers.

   b) If the preceding route is non-cooperative (i.e. h_2=0), when h_1 is transmitting with energy E_T and according to (6.3)-(6.5) and (6.6), identify all the nodes of which the SINR requirements of their transmitted packets can be reached (i.e. nodes that successfully overhear the signal intended for m from h_1). The effects of shadowing and multipath fading are not considered.

   c) If the preceding route is cooperative (i.e. $h_2 \neq 0$), when h_1 and h_2 are sending with energy βE_T and $(1-\beta)E_T$ respectively and according to (6.3),

(6.4), (6.6) and (6.19), identify nodes of which the SINR requirements of their transmitted packets can be reached. The effects of shadowing and multipath fading are not considered.

d) Nodes, whose SINR requirement of their transmitted packets can be reached as described in steps b and c, are put into the set **D**. However, set **D** excludes all nodes in the single path route and nodes that have already engaged in cooperation.

5. **(Ordering)** Arrange **D** in ascending order in distance to t.

6. **(Decide if cooperation should be done)**

a) Take out the 1st element from **D** and name it g (i.e. the element closest to t).

b) If $|\text{dist}(g,t) - \text{dist}(m,t)|/\text{dist}(m,t) \leq 0.5$, then g should cooperate with m and transmit to t. We update the cooperative route by putting g below m in matrix **C**. For example, if node 5 should cooperate with node 2 and transmit message to node 3 in this hop, then we have $C = \begin{pmatrix} 1 & 2 & 3 & 4 \\ 0 & 5 & 0 & 0 \end{pmatrix}$

c) If dist(m,t) $\geq$ dist(g,t), then g should cooperate with m and transmit to t. We update the cooperative route as in step 6b.

d) Otherwise, no cooperation. According to the order in **D**, try another node and name it g again. Repeat steps 6b-6d until the entire set **D** has been visited.

After finishing step 6, loop back to step 3 until the whole route has been visited.

In steps 4b and c, the set **D** obtained may be potentially different from each other. For example, node b in Fig. 6.4 has a higher possibility to overhear the message than that in Fig. 6.3, while node a is likely to overhear the messages in both scenarios.

Considering step 6b, when the power distribution ratio β is set to be 0.5, the outage performance would be optimal when dist(m,t) = dist(g,t). This step ensures that cooperation should only occur if dist(m,t) and dist(g,t) are comparable in length for good outage performance. However, in situation where the difference between dist(m,t) and dist(g,t) is large (say dist(m,t) $\ll$ dist(g,t)), it is better to allocate all the transmit energy to node m than to let node m cooperate with node g, since negligible signal energy would be received by the transmission from node g compared with that from node m. Step 6c means that a node g should always cooperate with node m if it can overhear the signal from h_1 (or h_2 if exists), and that it is situated closer to node t than node m. The additional transmission from node g increases both the diversity order and the average received signal energy at the receiver.

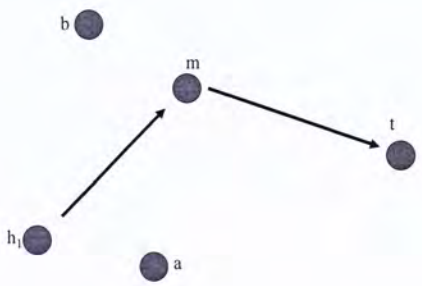

Figure 6.3: Notation used in our algorithm when the previous hop is non-cooperative.

6.4 Performance Evaluation

Consider a grid network which the positions of the relay nodes and interferers are shown in Fig. 6.5. Suppose the source and sink are nodes 1 and 19 respectively. A

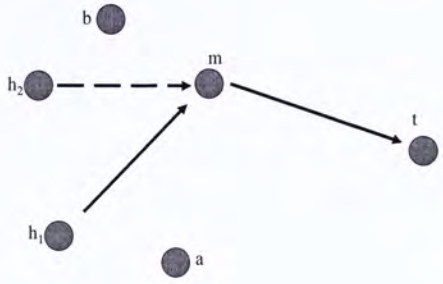

Figure 6.4: Notation used in our algorithm when the previous hop is cooperative.

long hop routing algorithm is used to generate the single path route first. Long hop routing is chosen because more relay nodes can potentially "overhear" the signal, and thus increases the chance of cooperation. In this routing algorithm, a node chooses to forward packets to the node that is within its transmission range R and is closest to the destination. Using $R = 7.5$m, the single path $\mathbf{S} = [1\ 5\ 10\ 14\ 19]$ is chosen. Applying our Cooperative Routing Algorithm as discussed in the previous section, we obtain the cooperative route $C = \begin{pmatrix} 1 & 5 & 10 & 14 & 19 \\ 0 & 2 & 7 & 11 & 0 \end{pmatrix}$. It means that besides the transmission in single path route, node 2 (who can "overhear" the signal from node 1 intended to node 5) should cooperate with node 5 to transmit to node 10; node 7 should cooperate with node 10 to transmit to node 14 and node 11 should cooperate with node 14 to transmit to node 19.

We then evaluate the performance of the three transmission strategies, namely 1) No Cooperation; 2) Simple Cooperation; 3) Cooperation with Interference Cancellation. Schemes 2 and 3 use the same route $\mathbf{C}$ but their reception statistics are

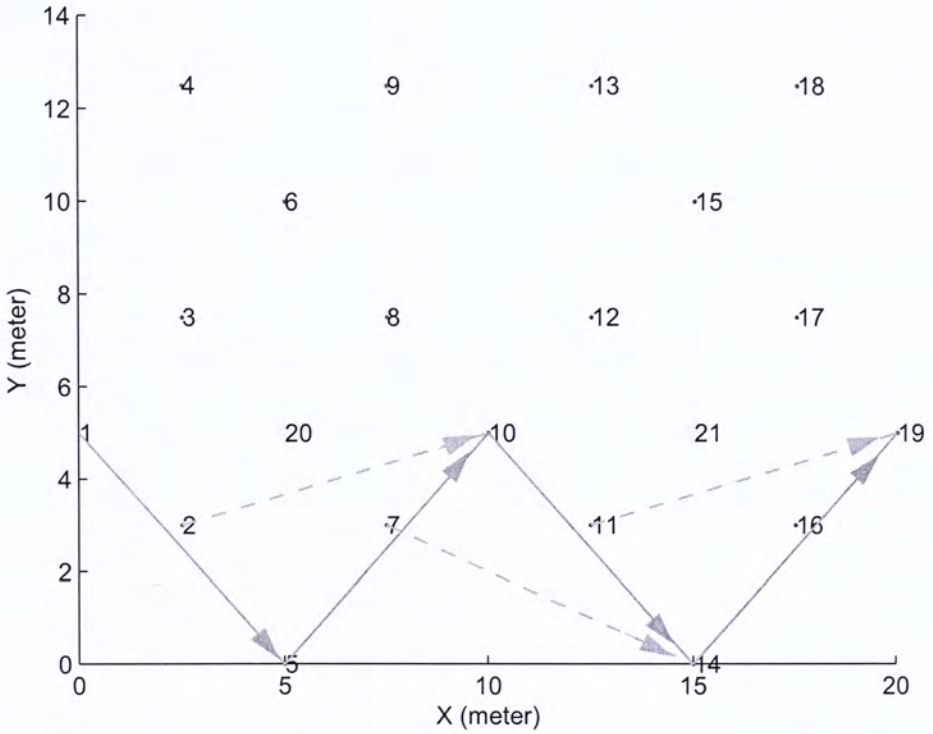

Figure 6.5: Network used in our simulation. The circles represent the possible relay nodes and the two diamonds (nodes 20 and 21) are interferers. The solid lines represent the transmissions in the original single path route, while the dotted lines represent the additional transmissions during cooperation.

different. The following parameters are used in our simulation:

- Transmitted signal: PPM-TH-UWB
- Receiver: Partial Rake, which captures the first three arriving multipath components at the receiver input.
- Received pulse $p(t) = [1 - 4\pi(t/t_n)]\,[\exp(-2\pi(t/t_n)^2)]$ with $t_n = 0.7531ns$ and pulse width $T_p = 2ns$.
- Power distribution ratio $\beta = 0.5$.
- Total number of nodes = 21.
- Total number of interferers = 2.
- Data rate per hop = 0.1Mbps.
- BER requirement = 1×10^{-3}.
- Frame duration $T_f = 5ns$.
- $\sigma_M^2 = 4.55 \times 10^{-9}$.
- Reference gain at a 1m: $c_0 = 10^{-4.7}$ and path loss exponent $\gamma = 1.7$ for multipath-affected channels with Line of Sight (LOS) over short distances [27].
- Noise power spectral density $N_0 = 4 \times 10^{-20}$W/Hz.

We define an outage on the route as when any of the hops along it cannot reach the SINR required to achieve the BER. In our evaluation, given a certain transmit SNR ζ for the route (x-axis in Fig. 6.6), the transmit SNR ϵ for the sender in each hop is obtained by dividing ζ by the total number of hops. We assume that all the interferers are transmitting at the same level as the relay nodes. In each iteration, we evaluate hop by hop from the source to the sink. For each hop, we evaluate the three transmission strategies with different ϵ, using the same set of channel condition. After running 10000 iterations for different channel conditions, the result

is shown in Fig. 6.6. From the figure, we see that at 3% of outage, our cooperative schemes requires 8dB less transmit energy than the non-cooperative one. Moreover, the non-cooperative scheme cannot reach an outage performance lower than 2%.

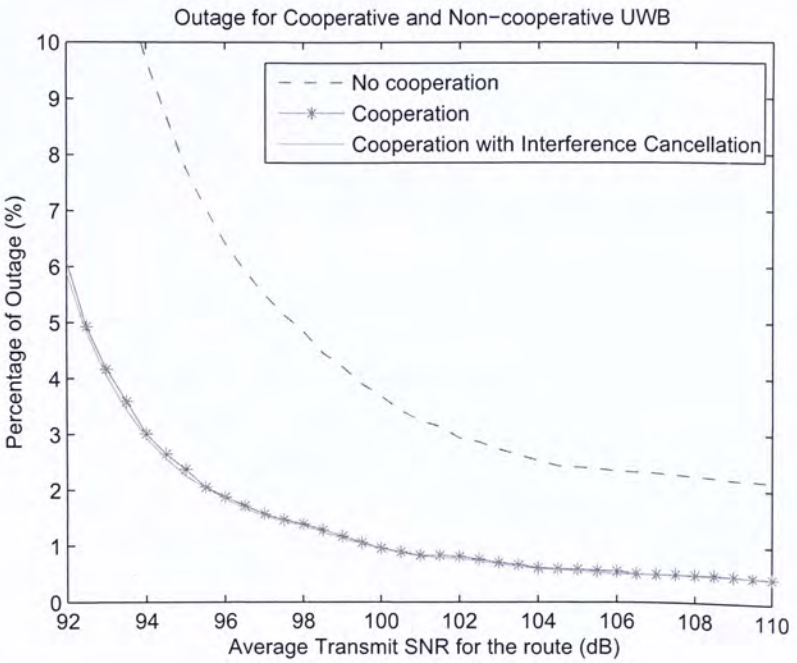

Figure 6.6: Outage performance for the three schemes against different levels of transmit SNR.

□ **End of chapter.**

Chapter 7

Conclusion and Future Work

7.1 Conclusion

In this thesis, we study energy-efficient routing based on physical layer models of Rayleigh fading channel and PPM-TH-UWB. Given a certain performance requirement (such as bit error rate (BER) or probability of outage), we are interested to find routing and transmission strategies that minimize the energy consumption.

In chapter 3, we study cooperative routing in Rayleigh fading channel. We have determined the criteria for cooperation and the optimal power distribution factor β that minimizes the probability of outage. Performance analysis and simulation of the scheme are performed on a 1D Poisson random network and a 2D grid network. Cooperative routing algorithm is suggested and is evaluated in 2D random networks. It is shown that the cooperative schemes achieve a diversity order of two.

In chapter 4, we derive the BER performance for PPM-TH-UWB systems under AWGN and MUI using Rake receiver, which serves as the cornerstone for the following chapters. In chapter 5, we study Interference-Aware Routing in UWB networks. We have proposed a link cost for energy-efficient routing based on the above BER expression. Then, we introduce an optimal interference-aware routing algorithm, which can find the least energy-consuming path in routing data packets from source

to destination, and at the same time achieve the BER requirement. A simplified version of this algorithm is also introduced. It has been shown that our schemes consume less energy in many cases as compared to some simple routing algorithms, such as long-hop, short-hop and location-based routing in a network with random topology.

In chapter 6, we study Cooperative Routing in UWB networks. We have described three different transmission strategies in a network and have shown the potential benefit of cooperative routing in an environment with both MUI and fading. We have proposed a Cooperative Routing Algorithm to improve the outage performance for a given single path route. Performance evaluation is given for a grid network. It is shown that our cooperative schemes reduce the average transmit energy in order to achieve a certain outage performance in a particular UWB grid network.

It should be noted that the cooperative routing and interference-aware routing tackle problems in different setup, although they both consider the effect of MUI. In interference-aware routing, we consider the long term average of the channel and only the effect of path loss is studied. In cooperative routing, the effects of path loss, shadowing and multipath fading are taken into account. The performance measure is BER in interference-aware routing, while that it is probability of outage in cooperative routing. In interference-aware routing, only the positions of source and destination are given. However, in cooperative routing, a single path route has already been formed.

7.2 Future Work

Cooperative communications and routing are hot research topics recently. Some of the interesting extensions for our future work are shown below:

7.2.1 Distributed Algorithm

Our two-node Cooperative Routing Algorithm is a centralized algorithm which a network control centre computes all the paths. More effort can be paid to develop a distributed algorithm that the nodes perform their own routing computations. The algorithm can thus be applied easily in real-world wireless ad-hoc networks.

7.2.2 Performance Analysis in Random Networks

Our cooperative routing algorithms in chapter 3 and 6 have only been evaluated by simulation using some physical layer models. Mathematical analysis can be done to evaluate the performance analytically. Moreover, it may shed light on how to design a better routing algorithm based on the analytical results.

7.2.3 Cross-Layer Optimization

As our routing protocol is based on physical layer model, cross-layer optimization among the physical, MAC and networking layers may lead to a better performance. For example, we may consider the joint optimization of routing, scheduling and power control problem.

7.2.4 Game Theory

In our setup, we consider that all nodes are unselfish. They are willing to cooperate whenever other nodes request them to do so. However, in the real world, nodes in ad hoc networks are subject to limited power supply that they should utilize their power efficiently. Motivation must be provided for independent nodes to cooperate. Game theory is a good tool (e.g. [26] and [16]) to study the motivation and behaviour of nodes in ad hoc networks, which are decentralized and do not have any infrastructure. The results can then be used to develop a more comprehensive cooperative routing algorithm and protocol.

7.2.5 Other Variations in Cooperative Schemes

Since our cooperative scheme involves only two nodes and is quite simple, more complex cooperative schemes may be considered, such as if more than two nodes are allowed to cooperate or if space-time coding is applied. Moreover, the issue of coded cooperation by integrating cooperation into channel coding may be considered [30].

□ **End of chapter.**

Bibliography

[1] A. Abdrabou and W. Zhuang. A position-based qos routing scheme for uwb mobile ad hoc networks. *IEEE Journal on selected areas in commun.*, 24(4):850–856, Apr. 2006.

[2] P. Baldi, L. D. Nardis, and M.-G. D. Benedetto. Modeling and optimization of uwb communication networks through a flexible cost function. *IEEE Journal of Selected areas in commun.*, 20(9):1733–1744, Dec. 2002.

[3] R. G. Bartle and D. R. Sherbert. *Introduction to Real Analysis.* New York: John Wiley & Sons, 2000.

[4] M.-G. D. Benedetto and et al. *UWB communication systems : a comprehensive overview.* New York: Hindawi Pub. Corp., 2006.

[5] M.-G. D. Benedetto and G. Giancola. *Understanding Ultra Wide Band Radio Fundamentals.* Prentice Hall Pearson Education Inc, New Jersey, 2004.

[6] J. Boyer, D. D. Falconer, and H. Yanikomeroglu. Multihop diversity in wireless relaying channels. *IEEE Trans. on Commun.*, 52(10):1820–1830, Oct. 2004.

[7] M. Canales, J. R. Gallego, A. Hernandez-Solana, and A. Valdovinos. Interference-aware routing with bandwidth requirements in mobile ad hoc networks. In *Proc. IEEE VTC 2005 Fall*, pages 2556–2560, Sept. 2005.

[8] D. Cassioli, M. Z. Win, and A. F. Molisch. Effects of spreading bandwidth on the performance of uwb rake receivers. In *Proc. IEEE ICC 03*, Mar. 2003.

[9] S. H. Chen, U. Mitra, and B. Krishnamachari. Invited paper: cooperative communication and routing over fading channels in wireless sensor networks. In *International Conference on Wireless Networks, Communications and Mobile Computing*, volume 2, pages 1477–1482, June 2005.

[10] M. H. Cheung and T. M. Lok. Interference-aware routing in uwb wireless networks. In *Proc. IEEE TENCON 06, Hong Kong*, Nov. 2006.

[11] M. H. Cheung and T. M. Lok. Cooperative routing in uwb wireless networks. In *Proc. IEEE WCNC 07, Hong Kong*, Mar. 2007.

[12] J. D. Choi and W. E. Stark. Performance of ultra wideband communications with suboptimal receivers in multipath channels. *IEEE Journal of Selected Areas in Commun.*, 20(9):1754–1766, 2002.

[13] G. B. Figueiredo, N. L. S. da Fonseca, and J. A. S. Monteiro. A minimum interference routing algorithm. In *Proc. IEEE ICC*, June 2004.

[14] B. Gui, L. Dai, and L. J. Cimini. Routing strategies in multihop cooperative networks. In *Proc. IEEE WCNC 07, Hong Kong*, Mar. 2007.

[15] R. Gupta, Z. Jia, T. Tung, and J. Walrand. Interference-aware qos routing (iqrouting) for ad-hoc networks. In *Proc. IEEE GLOBECOM'05*, Dec. 2005.

[16] R. Gupta and A. K. Somani. Game theory as a tool to strategize as well as predict nodes' behavior in peer-to-peer networks. In *Proc. IEEE 11th Conf. Parallel and Distributed Systems*, pages 244–249, July 2005.

[17] M. Haenggi. Analysis and design of diversity schemes for ad hoc wireless networks. *IEEE Journal on Selected Areas in Commun.*, 23(1):19–27, Jan. 2005.

[18] M. Haenggi. On distances in uniformly random networks. *IEEE Trans. on Information Theory*, 51(10):3584–3586, Oct. 2005.

[19] G. Heijenk and F. Liu. Interference-based routing in multi-hop wireless infrastructures. *Springer*, pages 117–127, 2005.

[20] W. Horie and Y. Sanada. Novel routing schemes based on location information for uwb ad-hoc networks. *Wiley Periodicals, Electronic and Comm. in Japan, part 3*, 88(2):22–30, 2005.

[21] A. E. Khandani, E. Modiano, J. Abounadi, and L. Zheng. Cooperative routing in wireless networks. *Advances in Pervasive Computing, Springer, US*, pages 97–117, 2005.

[22] M. S. Kodialam and T. V. Lakshman. Minimum interference routing with applications to mpls traffic engineering. In *Proceedings of INFOCOM (2)*, pages 884–893, Mar. 2000.

[23] S. Kwon and N. B. Shroff. Energy-efficient interference-based routing for multihop wireless networks. In *Proc. IEEE INFOCOM'06, Barcelona, Spain*, pages 1–12, Apr. 2006.

[24] J. N. Laneman, D. N. C. Tse, and G. W. Wornell. Cooperative diversity in wireless networks: efficient protocols and outage behavior. *IEEE Trans. Inf. Theory*, 50(12):3062–3080, Dec. 2004.

[25] J. N. Laneman and G. W. Wornell. Energy efficient antenna sharing and relaying for wireless networks. In *Proc. WCNC 2000, Chicago, IL, USA*, pages 7–12, Sept. 2000.

[26] A. B. MacKenzie and S. B. Wicker. Game theory in communications: Motivation, explanation, and application to power control. In *Proc. IEEE GLOBECOM'01, San Antonio, TX, USA*, pages 821–825, Nov. 2001.

[27] A. F. Molisch, J. R. Foerester, and M. Pendergrass. Channel models for ultrawideband personal area networks. *IEEE Wireless Communications*, 10:14–21, 2003.

[28] L. D. Nardis, P. Baldi, and M.-G. D. Benedetto. Uwb ad-hoc networks. In *Proc. of IEEE Conference on Ultra Wideband Systems and Technologies*, pages 219–224, 2002.

[29] L. D. Nardis, G. Giancola, and M.-G. D. Benedetto. A power-efficient routing metric for uwb wireless mobile networks. In *Proc. IEEE Vehicular Technology Conference*, pages 3105–3109, 2003.

[30] A. Nosrantina, T. E. Hunter, and A. Hedayat. Cooperative communication in wireless networks. *IEEE Commun. Magazine*, pages 74–80, Oct. 2004.

[31] M. Pioro and D. Medhi. *Routing, Flow and Capacity Design in Communication and Computer Networks.* San Francisco: Morgan Kaufmann Publishers, 2004.

[32] J. G. Proakis. *Digital Communications.* McGraw Hill, 2001.

[33] R. C. Qiu, H. Liu, and X. Shen. Ultra-wideband for multiple-access communications. *IEEE Commun. Magazine*, 43(2):80–87, Feb. 2005.

[34] B. Radunovic and J.-Y. L. Boudec. Optimal power control, scheduling, and routing in uwb networks. *IEEE J. Selected Areas in Communications*, 22(7):1252–1270, 2004.

[35] J. H. Reed. *An Introduction to Ultra Wideband Communication Systems.* New Jersey: Prentice Hall, 2005.

[36] A. Scaglione, D. L. Goeckel, and J. N. Laneman. Cooperative communications in mobile ad hoc networks. *IEEE Signal Processing Magazine*, 23(5):18–29, Sept. 2006.

[37] J. H. Schiller. *Mobile Communications.* Addison Wesley Longman, Inc., 2000.

[38] R. A. Scholtz. Multiple access with time-hopping impulse modulation. In *Proc. MILCOM'93*, pages 447–450, Oct. 1993.

[39] A. Sendonaris, E. Erkip, and B. Aazhang. Increasing uplink capacity via user cooperation diversity. In *Proc. ISIT, Cambridge, MA, USA*, page 156, Aug. 1998.

[40] A. Sendonaris, E. Erkip, and B. Aazhang. User cooperative diversity - part i: system description. *IEEE Trans. Commun.*, 51:1927–1938, Nov. 2003.

[41] A. Sendonaris, E. Erkip, and B. Aazhang. User cooperative diversity - part ii: implementation aspects and performance analysis. *IEEE Trans. Commun.*, 51:1939–1948, Nov. 2003.

[42] M. K. Simon. *Probability Distributions Involving Gaussian Random Variables: A Handbook for Engineers and Scientists.* Massachusetts: Kluwer Academic Publishers, 2002.

[43] M. K. Simon and M. S. Alouini. *Digital Communication over Fading Channels: A Unified Approach to Performance Analysis.* John Wiley and Sons, New York, 2000.

[44] B. Sklar. Rayleigh fading channels in mobile digital communication systems part i: characterization. *IEEE Communications Magazine*, 35(7):90–100, July 1997.

[45] L. Song and D. Hatzinakos. Cooperative transmission in poisson distributed wireless sensor networks: protocol and outage probability. *IEEE Trans. in Wireless Commun.*, 5(9):2834–2843, Oct. 2006.

[46] J. Tang, G. Xue, C. Chandler, and W. Zhang. Interference-aware routing in multihop wireless networks using directional antennas. In *Proc. IEEE INFOCOM 2005*, pages 751–760, Mar. 2005.

[47] M. Z. Win and R. A. Scholtz. Impulse radio: how it works. *IEEE Commun. Letters*, 2(2):36–38, Feb. 1998.

[48] M. Z. Win and R. A. Scholtz. Ultra-wide bandwidth time-hopping spread spectrum impulse radio for wireless multiple-access communication. *IEEE Trans. Commun.*, 48:679–690, Apr. 2000.

[49] Q. Wu, Y. Xiong, Q. Zhang, Z. Guo, X.-G. Xia, and Z. Li. Joint routing and topology formation in multihop uwb networks. *IEEE Journal on selected areas in commun.*, 24(4):843–849, Apr. 2006.

[50] J. Xu, B. Peric, and B.Vojcic. Energy-aware and link adaptive routing metrics for ulta wideband sensor networks. In *Proc. 2nd International Workshop on Networking with Ultra Wide Band and Workshop on Ultra Wide Band for Sensor Networks*, pages 1–8, July 2005.

[51] L. Yang and G. Giannakis. Ultra-wideband communications - an idea whose time has come. *IEEE Signal Processing Magazine*, 21(6):26–54, Nov. 2004.

[52] W. Zhuang, X. Shen, and Q. Bi. Ultra-wideband wireless communications. *Wireless Commun. and Mobile Comp*, 3:663–685, Sept. 2003.